International Journal of Thermofluids 10 (2021) 100080

Contents lists available at ScienceDirect

International Journal of Thermofluids

journal homepage: www.elsevier.com/locate/ijtf

Comprehensive numerical model for the analysis of potential heat recovery solutions in a ceramic industry

M. Venturelli[a], D Brough[b], M. Milani[a], L. Montorsi[a,*], Hussam Jouhara[b]

[a] Department of Sciences and Methods for Engineering, University of Modena and Reggio Emilia, Reggio Emilia, Italy
[b] Heat Pipe and Thermal Management Research Group, Brunel University London, Uxbridge, Middlesex, UB8 3PH London, UK

ARTICLE INFO

Article History:
Received 30 December 2020
Revised 9 March 2021
Accepted 10 March 2021
Available online 18 March 2021

Keywords:
Numerical model
Waste heat recovery
Energy efficiency
Ceramic industry
Environmental impact
TRNSYS

ABSTRACT

Heat recovery opportunities and total plant energy efficiency improvements need to be evaluated before manufacturing the real components when addressing the energy and economic effectiveness in industrial applications. Numerical modelling of the complete energy systems can be a key design tool in order to investigate the potential solutions to improve the performance of the considered system. In this study, a 0D/1D numerical analysis and transient system simulation analysis are adopted to investigate the energy efficiency enhancement given by the application of a heat pipe-based heat exchanger in the ceramic industry. The thermal power is recovered from the exhaust gases of the kilns used to fire the tiles. The numerical model includes all the main components of the heat recovery system: the primary side of the exhaust gases, the heat exchanger, the secondary circuit of the heat transfer fluid and the heat sink where the thermal power is exploited. Particular care is devoted to the modelling of the heat pipe-based heat exchanger and the necessary control strategy of the system; a specific model for the simulation of the secondary side pump is also accounted for in the analysis. The numerical results of the primary circuit are validated against experimental measurements carried out on the real ceramic facility. The good agreement between the numerical and experimental results demonstrates that the numerical model is an appropriate tool for investigating the energy efficiency enhancement of an industrial plant and for evaluating different configurations and solutions in order to fulfil the industry requirements.

Introduction

The application of waste heat recovery systems in an industrial context has recently attracted considerable interest due to the increasing consciousness of the potential impact of global warming in transforming our environment, the constant increase in fuel prices [1] and regulations and policies introduced to improve energy efficiency in industry [2,3]. Waste heat recovery from exhaust streams is one of the key factors for businesses to be competitive in a continuously changing marketplace. Within this context, the ceramic industry can be considered suitable for this kind of application because it is characterised by energy intense processes and a considerable amount of waste heat is lost to the atmosphere; indeed, it has been estimated that only the Italian ceramic tile and refractory materials industry has an annual consumption of methane gas equal to 1.5 billion m^3 and an electricity demand of 1800 GWh [4]. Thus, the energy efficiency of the ceramic process can be improved by the use of waste heat recovery systems, which can reduce greenhouse gas emissions and primary energy costs.

In literature, Jouhara at al. [5] studied the application of the waste heat recovery systems in the iron and steel, food and ceramic industries; a comprehensive review of waste heat recovery methodologies was presented, and the advantages and disadvantages of the main techniques were evaluated. An accurate analysis of the potential waste heat technologies that are and can be applied to the aluminium industry was carried out by [6].

In the ceramic sector, different solutions for waste heat recovery from exhaust sources have been analysed and several measures and techniques that can be implemented in order to enhance the energy efficiency of the tile manufacturing process were reviewed in the report named: “Reference Document in the Ceramic Manufacturing Industry” [7]. One of the most practised techniques highlighted is the heat recovery from excess hot air produced by a kiln. The energy content within this hot air exhausted from the cooling zone of a roller kiln can be used for preheating the air for the drying stage by means of intermediate heat exchangers. A theoretical approach for the evaluation of the energy recovery due to the exploitation of the cooling gases in the exhaust chamber was presented in [8]. The study

* Corresponding author:
E-mail address: luca.montorsi@unimore.it (L. Montorsi).

https://doi.org/10.1016/j.ijft.2021.100080

Nomenclature

Acronym	Description
HPHE	Heat Pipe-Based Heat Exchanger
0D/1D	Zero Dimensional-One Dimensional
HVAC	Heating, Ventilation and Air Conditioning
NTU	Number of Transfer Units
q_{conv}	Convective heat exchange W
h_{conv}	Convective heat transfer coefficient $W/m^2.K$
$area_{conv}$	Convective heat exchange area m^2
T_{gases}	Temperature of the gases K
T_{wall}	Temperature of the wall K
Nu	Nusselt number Dimensionless
λThermal conductivity	Thermal conductivityW/m.K
D_h	Hydraulic diameter m
$q_{conduction}$	Conductive heat transfer rate W
$T_{layer\ N}$	Temperature of material layer, N K
$T_{layer\ N+1}$	Temperature of material layer, N+1 K
Area	Heat exchange area m
p_{out}	Output pressure bar
p_{in}	Input pressure bar
Δp	Pressure difference between p_{in} and p_{out} bar
P_{mech}	Power provided by the pump W
V	Volumetric flow rate m^3/s
f_{eff}Global efficiency of the pump	Global efficiency of the pumpDimensionless
Q_{max}	Maximum heat transfer rate in the heat exchanger W
$T_{hot,in}$	Temperature of the warm fluid at the inlet of the HE K
$T_{cold,in}$	Temperature of the cold fluid at the inlet of the HE K
$\dot{m}_{hot}$	Mass flow rate of the hot fluid at the inlet of the HE kg/s
$\dot{m}_{cold}$	Mass flow rate of the cold fluid at the inlet of the HE kg/s
R_{hot}	Thermal resistance at hot fluid level K/W
R_{wall}	Thermal resistance at wall level K/W
R_{cold}	Thermal resistance at cold fluid level K/W
Cp_{hot}	Specific heat capacity hot fluid J/kg.K
Cp_{cold}Specific heat capacity cold fluid	Specific heat capacity cold fluidJ/kg.K
ϵ	Thermal effectiveness of heat exchanger Dimensionless

quantified that the maximum potential energy savings in the kiln consumption was 17% per year by recovering energy from the cooling gas.

The second strategy commonly used to enhance the energy efficiency of the process is the installation of cogeneration units as there is simultaneous demand of heat and electric power required for the industrial processes [9]. Organic Rankine Cycles have been adopted and applied to the ceramic process; for instance, in [10], an ORC system was used to recover heat from the indirect cooling section of the kiln to produce electricity. The analysis demonstrated that it is possible to recover 128.19 to 179.87 kW of thermal power, while the maximum electrical power is ranged between 18.5 and 21 kW. The maximum efficiency of the ORC system was 12.47%.

The accurate performance prediction of a proposed waste heat recovery system is fundamental in order to optimise the solution, study the integration in the existing industrial process and for the evaluation of the economics of the design. The design of waste heat recovery systems can be improved by adopting numerical tools to evaluate different solutions and configurations and for the investigation of the performance prior to the manufacture of the real system or modifying an existing plant [11]. Furthermore, the numerical analysis can be exploited to study the system behaviour under time dependent operating conditions or under critical situations that could potentially occur.

In literature, there are many examples of using a numerical approach for the simulation of thermo-hydraulic components or energy systems in general. For instance, in [12] a numerical approach was adopted for the investigation of the evolution of the temperature distribution and the thermo-mechanical stresses due to a liquid aluminium injection through a nozzle for a cogeneration system based on Al-H_2O reaction. In the field of industrial food processing, a numerical approach has been adopted to investigate the operating parameters of the fruit and vegetables drying process [13]. Bunyawanichakul et al. [14] investigated a pneumatic dryer plant for rice processing where heat and mass transfer has been modelled with a 0D/1D approach. Similarly, a 0D/1D steady state approach was used to analyse different thermal configurations of a thermoelectric generator for HVAC purposes [15]. Luo et al. [16] carried out a steady state numerical analysis for determining the energy efficiency enhancement obtained by the combined use of PV façade and solar cooling.

The performance of a lab-scale exhaust to water heat pipe-based heat exchanger (HPHE) was investigated in [17] by comparing the experimental results with the simulation results obtained by means of a transient numerical simulation model, TRNSYS. A reasonable agreement was demonstrated and the study predicted 33 months payback for a theoretical full scale unit. This paper presents work that builds upon this paper by coding a dedicated HPHE component; significantly more accurate than a standard library component provided by the TRNSYS software. Further studies conducted on air to water HPHE units for the purpose of waste heat recovery have been conducted by [18,19]. In [20], the heat recovery system for the post-combustion flue gas treatment in a coffee roaster plant is investigated using a lumped and distributed parameter numerical modelling.

In the field of the ceramic industry, Milani et al. developed a lumped and distributed parameter numerical model of an entire ceramic kiln to simulate the performance of the system under actual operating conditions [11]. Similarly, in [21], a combined theoretical and numerical approach was adopted in order to determine the thermal energy that can be recovered by the application of a HPHE to the cooling stack of the ceramic kiln. It was demonstrated that a reduction of approximately 110,600 Sm^3 per year of natural gas can be saved determining a reduction of 164 tonnes per year of carbon dioxide.

An additional study related to the ceramic sector was conducted by Gomez et al. [22]. The study numerically investigated the feasibility of substituting natural gas with syngas in ceramic furnaces. The numerical simulations, in this case a computational fluid dynamic approach, were used to determine the proper geometry for the syngas burner. Modelling and multi-criteria optimisation was used in [23] to simulate and optimise the application of a combined heat and power generation system to a tile manufacturing industrial process. The optimisation process was carried out considering energy, economic and environmental variables in the objective function; the designed parameters of the systems (number and capacity of the prime movers, heating capacity of the boiler and cooling capacity of the chiller) were determined with the numerical model. Finally, the numerical analysis has been adopted in [24] to investigate the thermal and fluid dynamic behaviour of a ceramic tile cooking roller kiln and combined with the analysis of the mechanical stresses formed in the final ceramic product. The 0D/1D model has been employed to determine the influence of the cooling temperature profile on the final residual stresses of the tiles. The study demonstrated that the

ideal cooking profile can be obtained in the real kiln by varying the operating parameters to obtain an improvement in the quality of the tiles.

This paper is part of the Horizon 2020 project ETEKINA (heat pipe technology for industrial applications) (www.etekina.eu). In this project, the goal is to recover over 40% of the waste heat contained in the exhaust streams of three different industrial contexts (aluminium, steel and ceramic sector) and to re-use the recovered thermal energy in the industrial processes in order to decrease their carbon emissions and increase process efficiencies [1]. This paper focuses on the ceramic industry and it investigates the application of a HPHE to a ceramic plant; the benefits gained by the HPHE installation in terms of energy efficiency improvement and in terms of environmental impact reduction of the ceramic process are determined by means of a lumped and distributed numerical modelling. A TRNSYS analysis was conducted, which shows the requirement for a system with more controls to reduce fluctuating conditions. Building upon this work, the 0D/1D model includes the entire heat recovery system which consists of the primary and secondary circuit. In particular, the primary side of the system is composed by the waste heat source that is the exhaust gases of ceramic furnaces. The heat recovery unit, i.e. HPHE, is considered in the model to simulate the thermal power recovered to the heat transfer fluid, which is the secondary stream of the circuit modelled. Water is pumped in the secondary circuit as heat transfer fluid; the numerical model of the secondary side accounts for a specific model for the simulation of the pump and for the heat sink where the thermal power recovered is exploited. Experimental data (temperatures and flow rate of the primary side) are used as boundary conditions for the simulation of the heat recovery system performance to assess the stability of the designed control strategy of the system. The numerical results related to the thermal losses along the exhaust piping are validated against experimental data while the thermal performance of the entire heat recovery system numerical model is validated against theoretical correlations under nominal conditions.

The adoption of the HPHE in order to recover the heat from the exhaust gases of the tile firing process of ceramic furnaces reduced the fuel consumption by approximately 40% with respect to the system in its current layout, i.e. without heat recovery. The simulation demonstrated that the designed control strategy is reliable in order to keep the operating parameters in the desired range. Indeed, the 0D/1D model has been used to investigate the fluid dynamic behaviour of the entire heat recovery system; the simulations performed have enabled to test the influence of the control strategy parameters on the thermal performance of the heat recovery system when different phenomena could take place, such as the excess or the decrease of thermal energy available in the exhaust and the decrease of thermal energy required by the heat sink process. Finally, the designed control strategy response has been analysed simulating real fluctuating conditions detected by the installed sensors. The numerical analysis has been conducted in a reasonable time and with acceptable computational effort. Therefore, the 0D/1D model is a valuable tool for tuning the control strategy and for tailoring its parameters to maintain the desired working conditions of the system, reducing remarkably time and costs. The simulations provide the opportunity to investigate different working points of the system that, otherwise, would have analysed by experimental tests.

Test case

The heat recovery closed loop circuit simulated in this study is a system that will be installed within the Etekina project in a real ceramic tile production facility located in the ceramic district in Emilia Romagna, Italy. The ceramic process starts with a selection of the raw materials (mainly clays, feldspars, sands, kaolin) and they are grinded in continuous mills with a mixture of water. Secondly, hydraulic presses are used to mechanically compress the paste in order to create ceramic ware with a regular geometry; the tile body are then dried in order to reduce the water content, they are decorated and finally fired in ceramic furnaces at approximately 1250°C, see Fig. 1. Focusing on the thermal energy consumption of the ceramic process, the firing stage is responsible for approximately the 53% of thermal consumption, followed by the spray drying (35%) and drying (10%) [25].

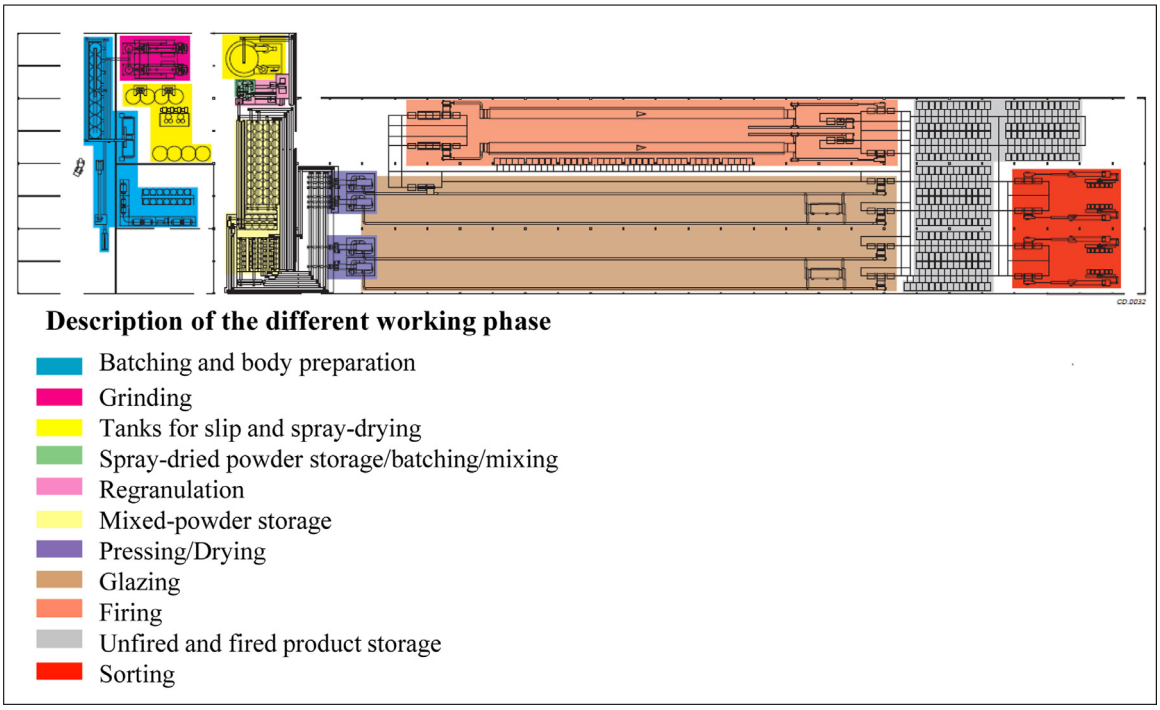

Fig. 1. Stages of the ceramic tile manufacturing process.

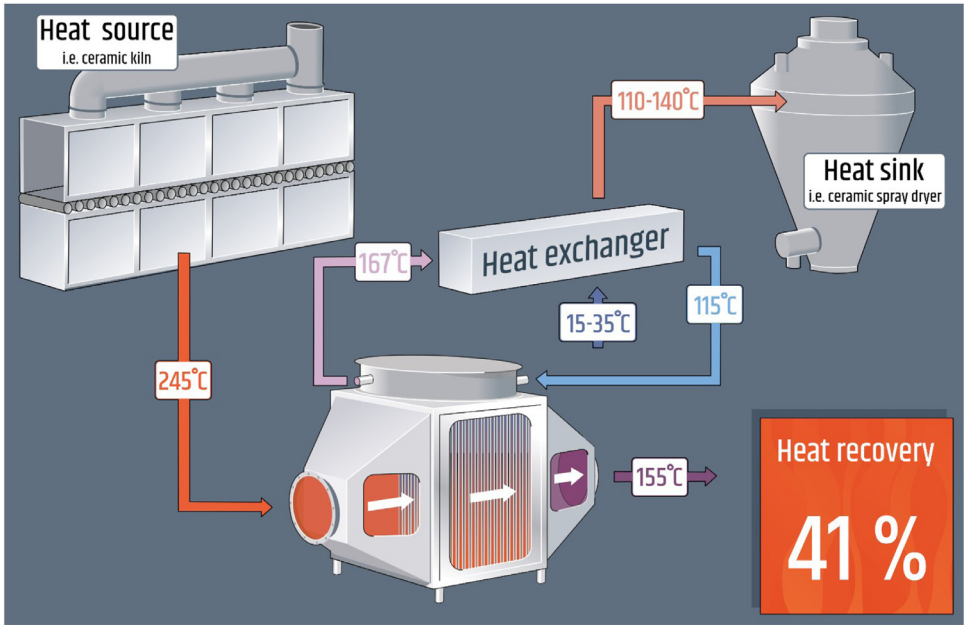

Fig. 2. Schematic of the designed heat recovery system.

In the Etekina project, the exhaust gases of firing kilns have been selected to be the heat source for the waste heat recovery since they are a potential source of high specific enthalpy and they are characterised by traditionally difficult to recover temperatures and flow rates (220-250°C, 10,000-15,000 Nm^3/h per kiln) with a high particulate content and also the presence of corrosive condensable gases. Thus, a HPHE will be installed in the ceramic facility before the main stack and the recovered heat from the exhaust gases of the furnaces will be transferred via a thermo-vector fluid, i.e. water, to the spray dryer. The heat recovered by the water will be transferred to the air used in the spray dryer by means of two intermediate heat exchangers positioned in parallel. This heat recovery reduces the spray dryer natural gas consumption by approximately 40%.

Fig. 2 shows the sketch of the heat recovery system layout representing the main designed operating parameters: in a regime working cycle, the exhaust gases are cooled down from the temperature of 245°C at the inlet of the HPHE to approximately 155°C, i.e. at the outlet of the heat exchanger; in the secondary side, the heat transfer fluid will benefit of approximately 50°C of delta temperature, since the designed temperature at the inlet of the system is 115°C while at outlet of the system is 165°C.

In the real facility, the existing primary side, i.e. the exhaust circuit, is equipped with different sensors that monitor the main operating parameters, which are temperatures, pressures, and flow rates. The sensors monitor the parameter values at a sampling rate of 15 minutes. The sensors installed are listed in Table 1 with their locations shown in Fig. 3. The sensors provide a complete characterisation of the fluid dynamic behaviour of the exhaust gases; indeed, different thermocouples are installed along the piping in order to monitor the thermal losses in the main section of the pipeline and across filter component. In the designed heat recovery configuration, the HPHE will be installed before the filter to increase the temperature of the exhaust gases at the inlet of the system in order to increase the amount of waste heat that can be recovered.

A detailed control strategy has been designed to keep under control the main operating parameters of the heat recovery system: the outlet temperatures at the HPHE, i.e. temperature of the exhaust gases (primary side) and temperature of the water (secondary side), which are respectively 155°C and 165°C. In particular, the heat transfer fluid circuit is equipped with a pump and an inverter in order to vary the flow rate of the water fluid; the desired temperatures at the outlets of the heat exchanger are maintained by varying the speed of the pump.

This study focuses particularly on the development of a 0D/1D numerical model for the simulation of the entire heat recovery system. Firstly, the numerical model of the primary side is developed for the simulation of the heat losses along the exhaust piping; the numerical results are compared and validated against experimental data available from the sensors. The lumped and distributed analysis is then improved with the introduction of specific models for the HPHE and the secondary circuit of the heat transfer fluid. The numerical model is validated against theoretical correlations used to design the system. Table 2 lists the main operating parameters of the designed heat recovery system. Finally, the numerical modelling is used to study the effects of the waste heat recovery and the response of the control strategy to working conditions that could occur in the real system; the time dependent simulations determine the working points of the heat recovery system for the tuning of the control strategy.

Materials and methods

HPHE numerical model

A TRNSYS model was developed to visualise the heat recovery profile from the exhaust with a fixed water mass flow rate and temperature. This was completed using the same methodology as [26] to determine the necessity for a control strategy. The component used

Table 1
Specification of the sensors installed.

Type of Sensor	Location	Reference
Temperature transducer	Beginning of the exhaust piping of the kiln#1	T1
Temperature transducer	Beginning of the exhaust piping of the kiln#2	T2
Temperature transducer	Manifold	T3
Pressure transducer	Manifold	P3
Temperature transducer	Filter inlet	T4
Pressure transducer	Filter inlet	P4
Temperature transducer	Filter outlet	T5
Pressure transducer	Filter outlet	P5
Pitot tube	Exhaust stack outlet	Q1

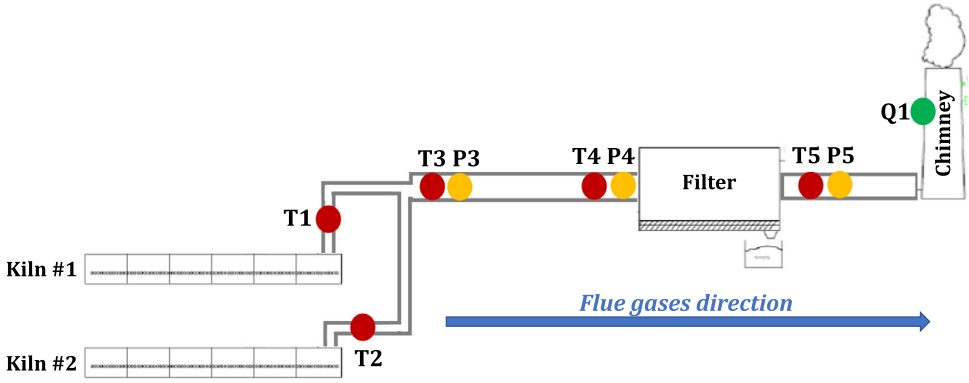

Fig. 3. Location of the sensors installed along the exhaust piping in the real facility.

Table 2
Operating parameters of the designed heat recovery system.

Design Parameters	Quantity
Exhaust Temperature HPHE inlet	245°C
Exhaust Temperature HPHE outlet	155°C
Water Temperature HPHE inlet	115°C
Water Temperature HPHE outlet	165°C
Thermal Power Recovered	700 kW

for the HPHE was a newly developed cross-flow component, instead of counterflow as done previously, reflecting the change in HPHE design. The mathematical code for the HPHE component was adjusted accordingly.

The HPHE unit

The HPHE modelled is an exhaust to pressurised water system (rated to 16 bar), Fig. 4 provides a general arrangement schematic. There are a total of 890 heat pipes with an active condenser length of 270 mm and an active vapourisation length of 2,655 mm. Fig. 5 provides a view of the 40mm thick separation plate and the spacing arrangement of the heat pipes. Table 3 provides the main design parameters of the HPHE unit.

TRNSYS simulation

Fig. 6 shows a view within the TRNSYS software of the model layout. Roughly 61 days of captured data of the exhaust temperature and mass flow rate were introduced into the HPHE. The sink stream was fixed at 115°C at a mass flow rate of 11,280 kg/hr as this was a suitable value for the plant. The outputs and the temperature inlet parameters were fed into graphical output components to visualise the outputs of the model. Table 4 provides a description of the components used and the identification of the component in TRNSYS.

Fig. 7 shows the predicted exhaust and water outlet temperatures of the HPHE as well as the inlet temperatures. The simulation predicts that there will be extreme fluctuations in outlet temperatures of the

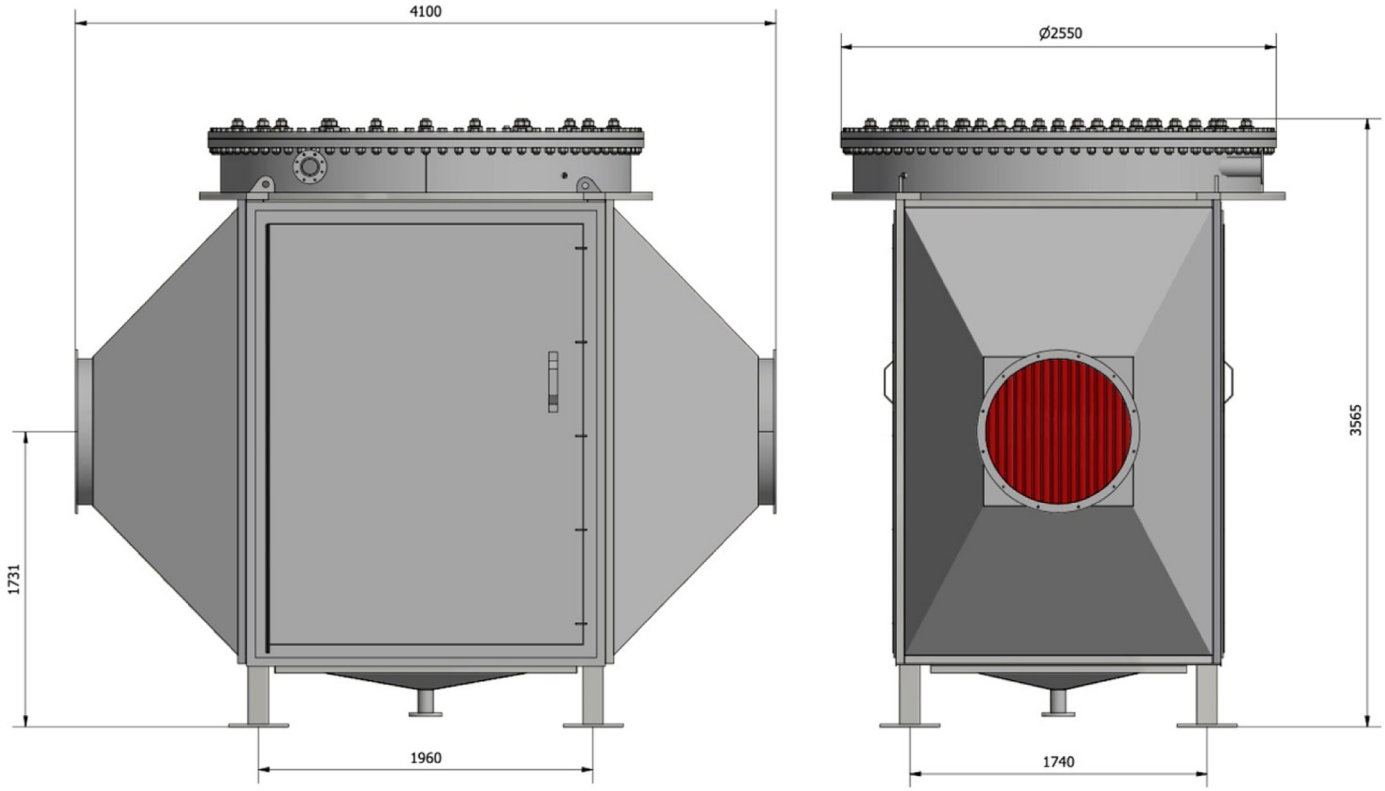

Fig. 4. General arrangement and sizing of HPHE.

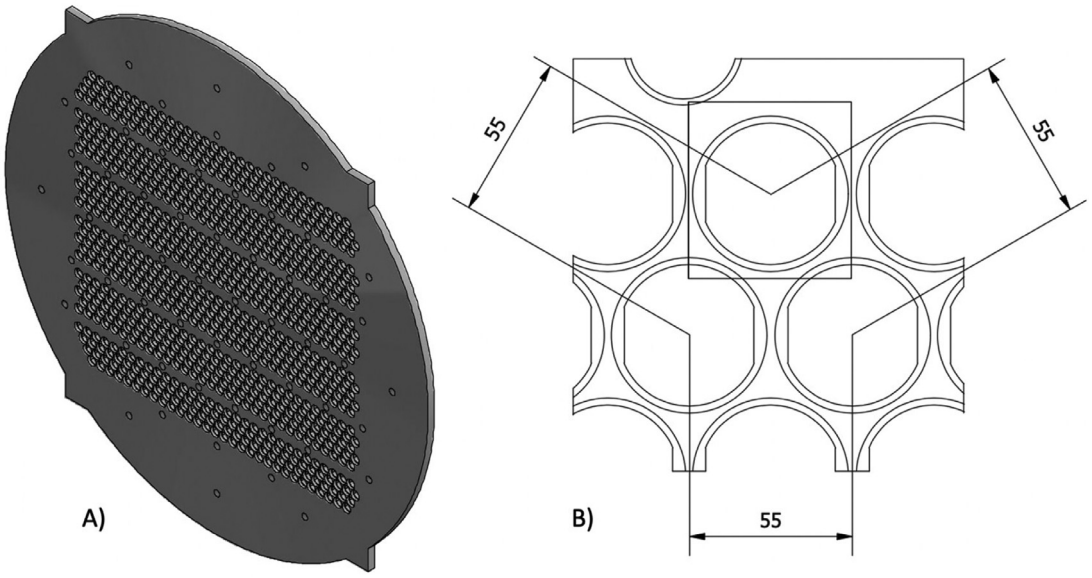

Fig. 5. A) HPHE separation plate. B) Equatorial spacing of heat pipes.

Table 3
HPHE Design Parameters.

Design Parameter	Value	Unit
Exhaust mass flow rate	26,000	kg/hr
Water mass flow rate	11,280	kg/hr
Exhaust average specific heat capacity	0.257	kcal/kg.°C
Water average specific heat capacity	1.000	kcal/kg.°C
Exhaust inlet temperature	245	°C
Exhaust outlet temperature	155	°C
Water inlet temperature	115	°C
Water outlet temperature	167	°C
Recovered heat	700	kW

water. The water is used to preheat air for a spray dryer. This process is critical to the quality of the end product and requires control and a relatively steady state. This graph shows that installing just a HPHE is not sufficient for this reuse of the recovered waste heat and a control strategy is needed to control the exhaust and water temperatures and the overall HPHE performance. The temperature of the water outlet fluctuated between 145 and 195°C. The exhaust temperature fluctuated between 125 and 170°C.

Fig. 8 shows the predictions for the energy recovery performance of the HPHE and the corresponding conductance (UA) value associated with the HPHE. The energy recovery ranged between 390 and 1080 kW and the conductance was between 12,800 and 16,500 W/K, ignoring a production stop that occurred within the data collection

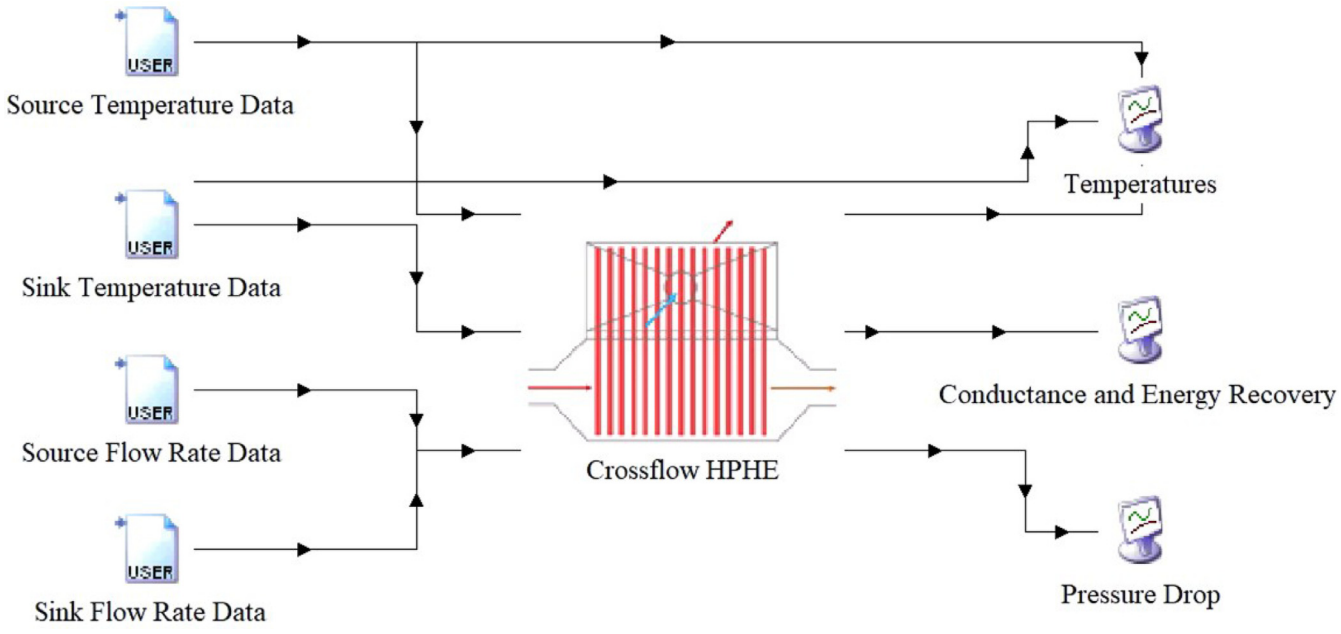

Fig. 6. Simulation Studio view of model.

Table 4
Icon, type number and description of the components used in the model.

Icon	Type Number	Description
	Type 9a	Data input file
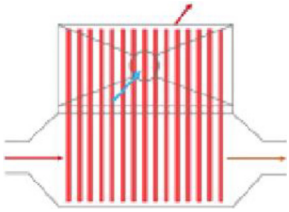	Type 204	User built crossflow HPHE
	Type 65d	Online graphical plotter to display outputs

period. Again, there is a high degree of fluctuation. With the determined end use of the waste heat being the spray dryer, control is required.

The HPHE model also gives outputs of pressure drop values, as shown in Fig. 9. This information is useful in sizing pumps and fans required to counteract these losses. The pressure drop of the exhaust reached up to 600 Pa for the evaporator section and was 1820 Pa for the water sink condenser section. However, the fluctuations are clear, highlighting the requirement of a control strategy, requiring variable speed pumps and valves to adjust the exhaust mass flow rate and hence energy content.

The results shown in Paragraph 3.1 demonstrate the need of a control strategy for the Etekina heat recovery circuit in order to control the fluctuating temperatures depicted in Fig. 7. The numerical model of the entire heat recovery system simulated in this study is developed by means of the software LMS Imagine.Lab AMEsim, licensed by Siemens [27].The heat recovery system includes three main sections: the exhaust circuit (primary side), the HPHE and the heat transfer fluid circuit (secondary side). The numerical model accounts for the pneumatic and thermal hydraulic libraries for the simulation of the exhaust gases and water circuit, respectively. In addition, the thermal library has been used to consider the solid parts of the circuits and their influence on the overall heat exchange.

The numerical model simulates the exhaust flow inside the primary piping accounting for the thermodynamic properties of the considered gas and the semi-perfect gases approach is accounted in the simulation. The numerical model of the exhaust circuit simulates the exhaust gases from the outlets of the ceramic kilns to the main stack; the input parameters are the flow rate and temperature of the gases measured by the sensors installed along the piping.

The heat recovery from the exhaust gases is transferred to the water flow by means of the HPHE located before the main stack; the waste heat recovery system is based on the heat pipe technology which uses the two-phase cycle (boiling and condensation) of a working fluid in order to transfer the heat from a hot stream to a cooler one. The HPHE system has been modelled in AMESim considering the heat pipes walls as superconductors using the values calculated in Fig. 7. Thus, a high value for the thermal conductivities of the evaporator and condenser sections of the heat pipes have been implemented in the software to account for the evaporation and condensation phenomena respectively.

The water of the secondary side is simulated using an available thermal-hydraulic library and the fluid properties (density, specific heat, dynamic viscosity, thermal conductivity) are modelled by polynomials of the pressure and temperature.

Fig. 10 shows the layout of the numerical model implemented in AMESim.

The focus of this analysis is the investigation of the whole thermal performance of the heat recovery circuit, as well as the evaluation of the effectiveness of the control strategy of the system in order to maintain the desired operating parameters under different working conditions, i.e. different flow rates and temperatures of the exhaust gases.

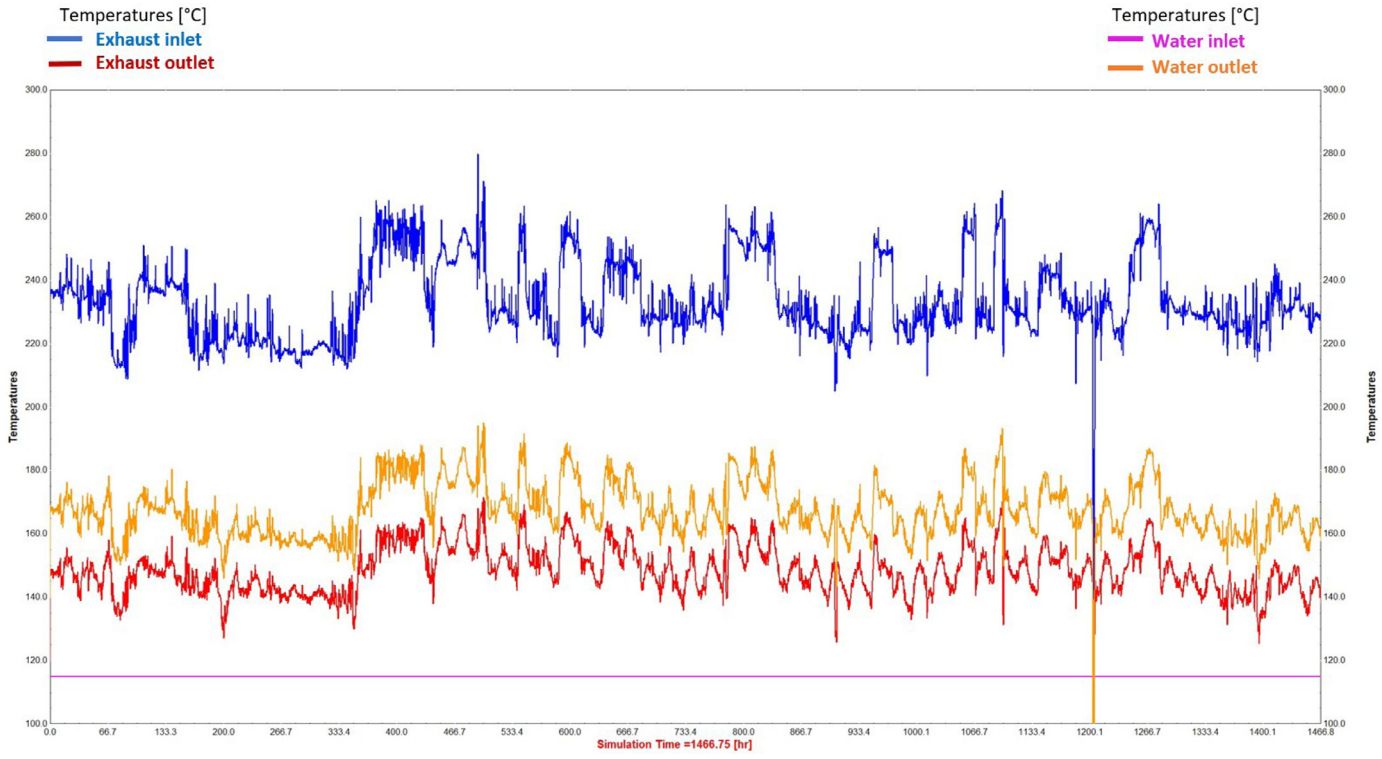

Fig. 7. Transient temperature performance of simulation.

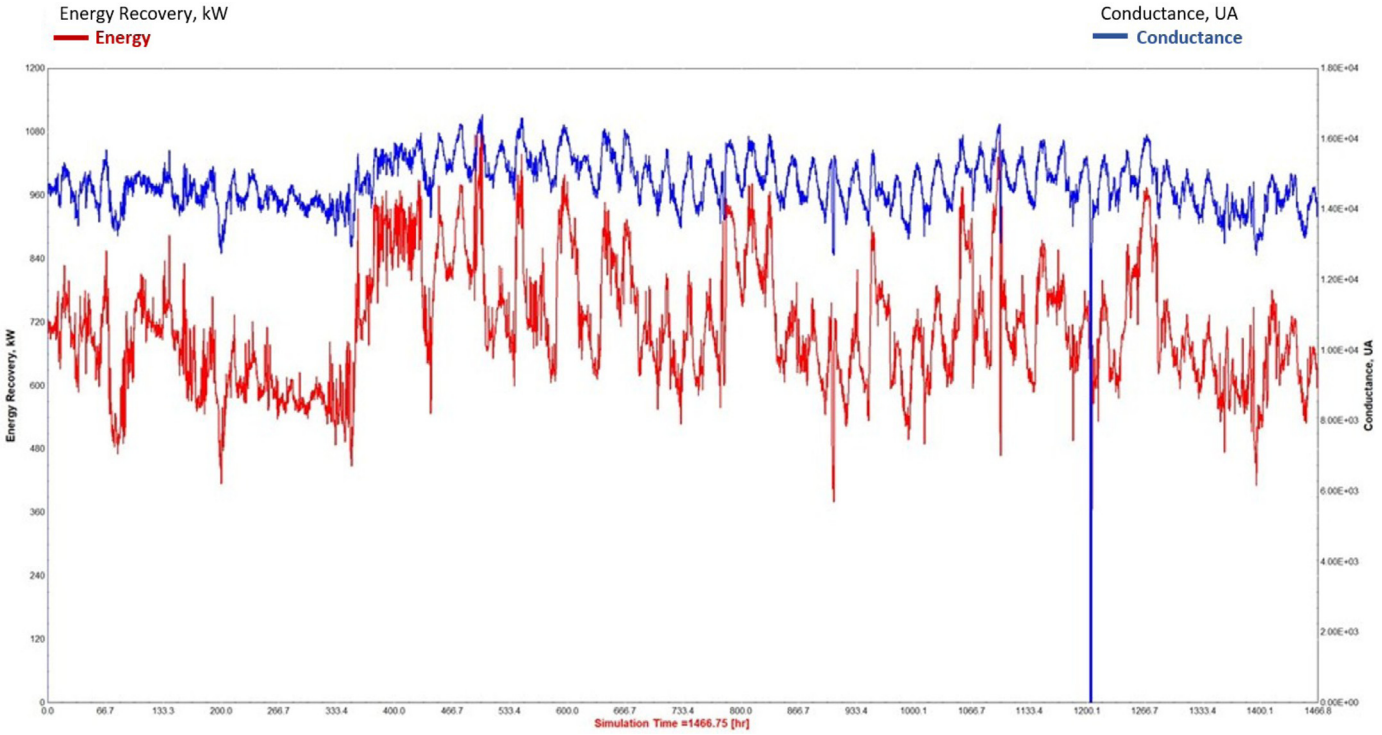

Fig. 8. Transient energy recovery and conductance of simulation.

In the model, particular care is devoted to the heat loss modelling of the exhaust and the water along the primary and secondary circuit respectively. Furthermore, specific models for the water pump and for the two intermediate heat exchangers that transfer the heat recovered by the water to the spray dryer are developed in the model. In the following, a description of the model adopted for the components displayed in Fig. 10 is presented.

Thermal losses of the primary and secondary side

As already mentioned, the numerical model developed accounts for the thermal losses in the exhaust and water circuit; the thermal exchange is considered between the fluid and an external ambient with an imposed temperature of 25°C.

The heat transfer between the fluid and the external ambient is composed by three contributions: convection between the fluid and

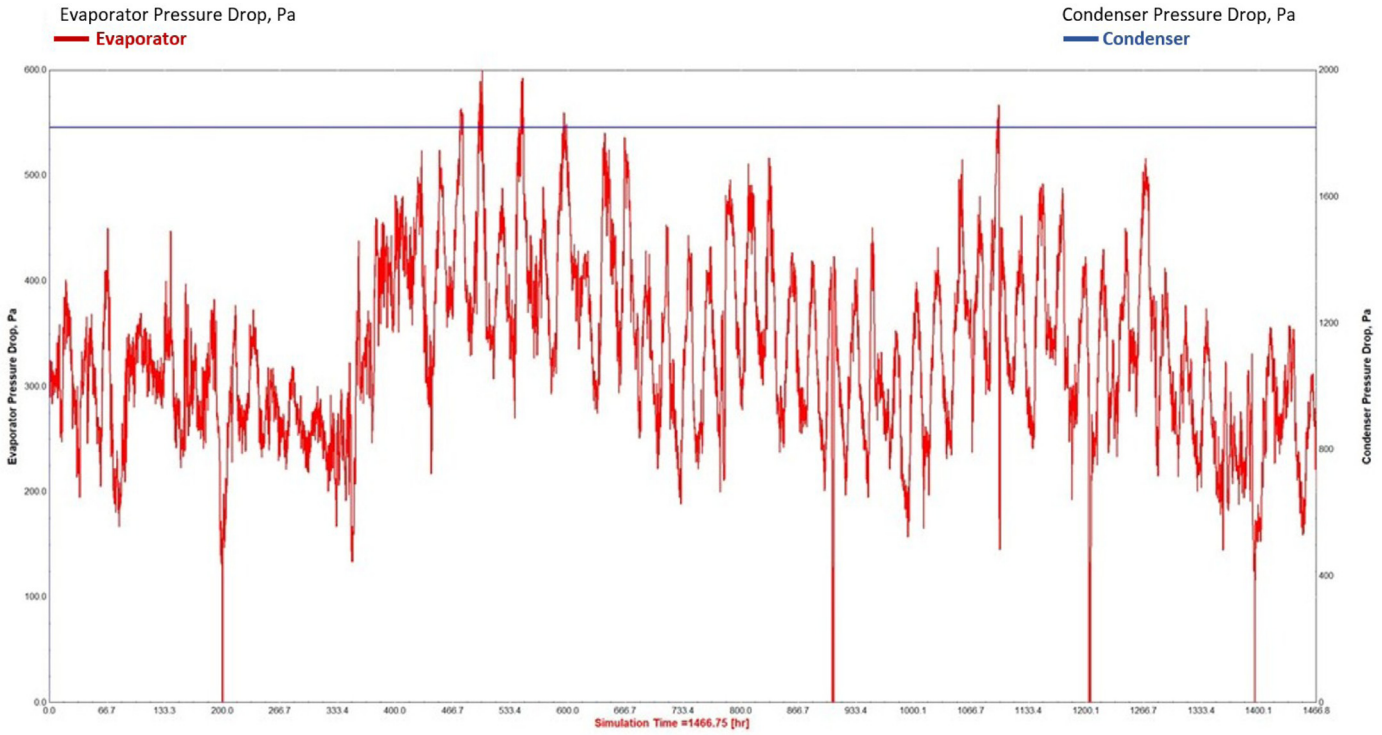

Fig. 9. Transient pressure drop predictions of simulation.Heat Recovery System Numerical Model

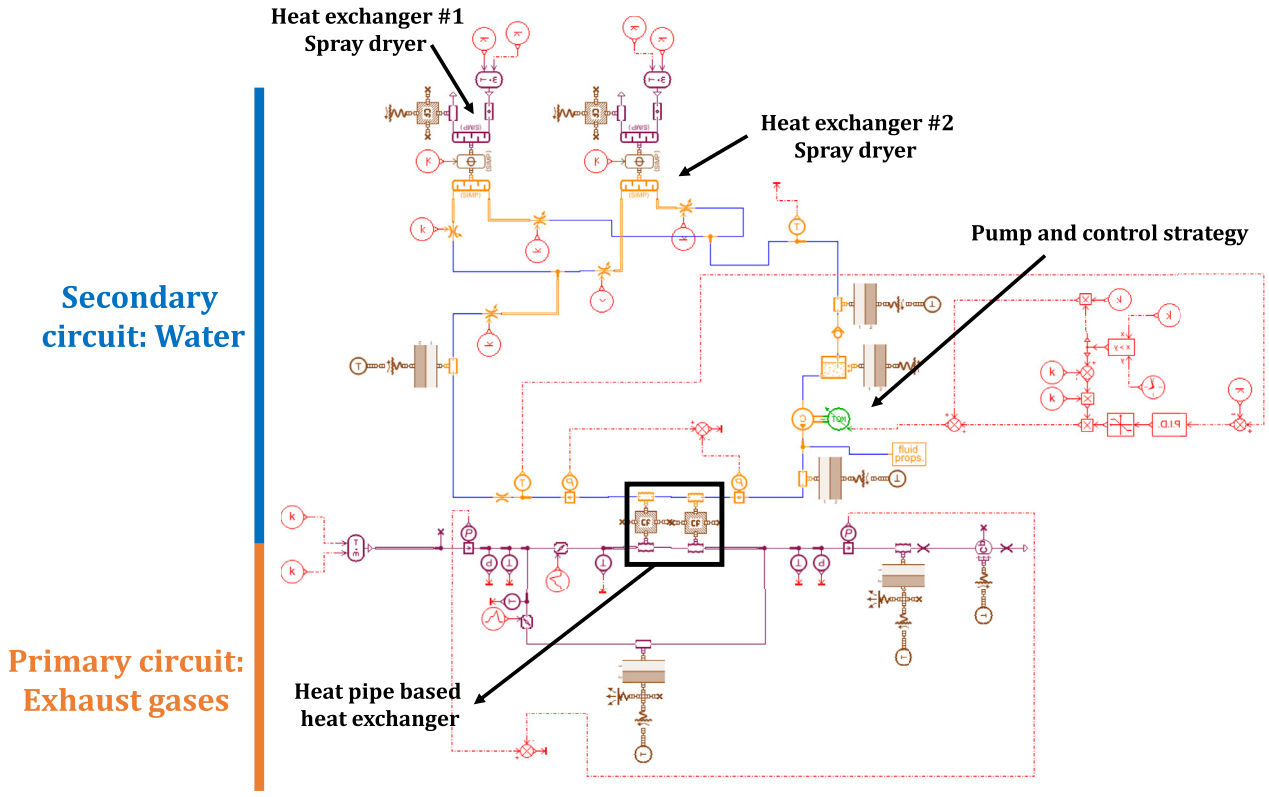

Figure 10: Layout of the numerical model of the whole heat recovery system.

Fig. 10. Layout of the numerical model of the whole heat recovery system.

the wall, conduction within the wall of the material and the external convection between the material and the external ambient. The first contribution, the convective heat exchange, q_{conv}, between the fluid, i.e. exhaust gases or water, and the material, i.e. wall of the pipe, is computed according to the following equation:

$$q_{conv} = h_{conv} * area_{conv} * (T_{gases} - -T_{wall}) \quad (1)$$

where $area_{conv}$ is the convective heat exchange area [m^2], T_{gases} and T_{wall} are, respectively, the temperature of the gases and the wall [K].

The heat transfer coefficient, h_{conv}, is calculated by:

$$h_{conv} = \frac{Nu * \lambda}{D_h} \quad (2)$$

where Nu is the Nusselt number, λ is the thermal conductivity of the fluid [W/m*K] and D_h is the hydraulic diameter [m].

In the case analysed, both the exhaust and the water piping are insulated; thus, the heat transferred by the conduction phenomenon within the walls of the pipes can be calculated according to:

$$q_{conduction} = \frac{T_{layer\ N} - T_{layer\ N+1}}{\frac{d_N}{Area*\lambda_N} + \frac{d_{N+1}}{Area*\lambda_{N+1}}} \quad (3)$$

where $T_{layer\ N}$ is the temperature of material layer N, d_N is the distance between temperature point of material layer N and temperature point of material layer N+1, Area is the heat exchange area and λ_N is the thermal conductivity of material layer N. The same definitions apply for the properties of material N+1.

Finally, the last contribution is the heat exchange between the piping walls and the external environment, which is calculated according to (Eq.1. The external ambient temperature is set equal to 25°C and the heat transfer coefficient is 6 W/m^2K, which is a standard coefficient of natural convection.

Water circuit

The secondary flow is pumped into the HPHE by means of a thermal-hydraulic centrifugal pump. The difference in pressure of the fluid passing through the pump is calculated using affinity laws. The fluid temperature at the pump outlet is calculated from the temperature at the pump inlet and the energy provided (with an overall efficiency) by the pump to the water. The characteristic curves (volumetric flow rate-pump head) have been implemented into the software for different velocities.

The mass flow rate at the suction of the pump is calculated so that the output pressure, p_{out} (high pressure), reaches the following value:

$$p_{out} = p_{in} + \Delta p \quad (4)$$

where p_{in} is the input pressure (low pressure) and Δp is the pressure difference. The pressure difference into the pump is interpolated thanks to the reference data.

The power, P_{mech}, provided by the pump to the fluid is as follows:

$$P_{mech} = V * \Delta p * f_{eff} \quad (5)$$

$$0 \leq f_{eff} \leq 1 \quad (6)$$

where V is the volumetric flow rate, Δp is the pressure difference and f_{eff} is the global efficiency of the pump.

The super-heated thermal fluid flows in the secondary piping toward the intermediate heat exchangers that transfer the recovered heat to the air required by the spray dryer process. The two heat exchangers are placed in parallel and they are designed to transfer 490 kW and 180 kW, respectively, to the air required by the spray dryer process. In the numerical model, the heat exchangers are modelled according to the efficiency-NTU method. A warm fluid with mass flow rate $\dot{m}_{hot}$ (kg/s) enters the heat exchanger at temperature

$T_{hot,in}$ (°C) and goes out the heat exchanger at temperature $T_{hot,out}$ (°C). Meanwhile a cold fluid with mass flow rate $\dot{m}_{cold}$ [kg/s] enters the heat exchanger at temperature $T_{cold,in}$ ◦9C) and leaves the heat exchanger at temperature $T_{cold,out}$ (°C). The heat transfer rate between the cold fluid and the hot fluid cannot exceed a maximum value Q_{max}. This value is given by:

$$Q_{max} = C_{min} * (T_{hot,in} - T_{cold,in}) \quad (7)$$

where C_{min} is the minimum heat flow rate capacity written as:

$$C_{min} = \min\left(\left|\dot{m}_{hot}\right| Cp_{hot} \left| \dot{m}_{cold} \cdot Cp_{cold}\right|\right) \quad (8)$$

The efficiency-NTU method states that the heat flux can be written as:

$$Q = \in * Q_{max} \quad (9)$$

where ε is the efficiency or thermal effectiveness of the heat exchanger. This thermal effectiveness can be written as a function of the number of transfer units, NTU, and the flow-stream capacity ratio, Cr:

$$\in = f(NTU, Cr) \quad (10)$$

NTU and Cr are defined as:

$$NTU = UA/C_{min} \quad (11)$$

$$Cr = C_{min}/C_{max} \quad (12)$$

where:

$$U * A = \frac{1}{R_{hot} + R_{wall} + R_{cold}} \quad (13)$$

$$C_{max} = \max\left(\left|\dot{m}_{hot}\right| \cdot Cp_{hot}, \left|\dot{m}_{cold}\right| \cdot Cp_{cold}\right) \quad (14)$$

R_{hot}, R_{wall} and R_{cold} are the thermal resistances, in K/W, at hot fluid level, wall level and cold fluid level, respectively.

Control strategy

In the numerical model, a temperature sensor is placed at the condenser outlet in order to measure the temperature of the water flow. A pump with variable rotational velocity from 1800 rpm to a maximum of 3000 rpm maintains the water stream at the desired temperature value of 167°C. Therefore, if the thermal power available in the exhaust stream is higher than the designed value, the pump increases the water flow rate in order to avoid the overheating of the water flow. In the event that this control strategy is inadequate for keeping the temperature at the desired value, the bypass of the HPHE in the primary side, i.e. exhaust, is partially opened to decrease the thermal power available in the gases. A total bypass of the HPHE primary side will be operated during downtime periods of the heat sink and during maintenance procedures.

Conversely, a decrease in the temperature or the flow rate of the exhaust gases at the inlet of the evaporator with respect to the designed values could lead to a decrease of the temperature of the exhaust at the outlet of the system; this condition must be avoided due to the acid condensate that could condense in the exhaust. As a consequence, in this scenario, the inverter decreases the speed of the pump to reduce the water flow rate. When the decrease of the thermal power available in the exhaust is significant, the control strategy activates a bypass of the intermediate heat exchangers in order to transfer less thermal power to the spray dryer. Thus, the heat recovered in the HPHE by the water will decrease allowing a higher temperature at the HPHE outlet to avoid dropping below acid condensation temperatures.

Experimental-numerical validation of the exhaust gases heat losses

As mentioned above, the first case is the simulation considering only the exhaust gases circuit, i.e. no heat recovery is considered in the simulation, in order to compare the numerical results with the experimental data. This simulation is useful to determine the gap between the experimental and numerical thermal losses along the exhaust piping. The experimental temperature and flow rate measured by the sensors at the manifold, see the sensors location in Fig. 3, are implemented in the numerical model as input parameters for the exhaust gases source. Fig. 11 shows the experimental values for temperature and flow rate collected over a period of approximately 2 days. The temperature measured at the manifold varies from a minimum of 210°C to a maximum of 260°C, while the flow rate has been normalized on the basis of its maximum value according to the following equation:

$$\text{Flow Rate}(\%) = (\text{Flow Rate}/\text{Flow Rate Max}) * 100 \quad (15)$$

The registered flow rate varies in the range from 40% to 100%.

Fig. 12 shows the comparison between the numerical and calculated temperature of the gases before the main stack, where the HPHE will be installed. The agreement between the numerical results and the experimental measurements is satisfactory, concluding that the thermal losses of the exhaust gases along the piping are predicted accurately. Indeed, the time-dependent temperature curves are aligned, and the difference is approximately 4-5°C; a maximum difference of 11°C can be noticed at approximately 50,000 and 75,000 seconds.

Numerical-theoretical validation of the entire heat recovery system

In the second simulation, the heat recovery system is introduced within the simulation. The HPHE and the closed loop heat transfer fluid circuit presented previously are included in the numerical model. The simulation has been carried out with the designed temperature and flow rate at the inlet of the exhaust piping and with the designed rotational speed of the pump, where the exhaust temperature is equal to 245°C and the pump rotational speed is equal to 2520 rpm. The initial temperatures of the materials components and of the water flow is 20°C. This simulation determines the deviation between the numerical results and the operating parameters of the designed heat recovery system, shown in Table 2, which are determined by theoretical correlations.

Fig. 13 displays the main numerical operating parameters of the system: the temperature of the exhaust gases at the outlet of the HPHE and the inlet and outlet temperatures of the water from the HPHE and the thermal power recovered by the heat exchanger. The warm-up phase of the water flow can be noticed at the beginning of the simulation: the water takes approximately 10,000 seconds to reach its steady value of 115.4°C. The water temperature at the outlet of the heat exchanger stabilizes at 166.7°C while the numerical temperature of the exhaust before flowing to the atmosphere is 155.5°C. These numerical results are very close to the designed parameters of the system reported in Table 2. The numerical thermal power recovered by the HPHE is reported in Fig. 13 and it is equal to 716,850 W. Therefore, the model predicts the energy recovery performance 2.4% higher than the manufacturers provided designed recovery power of 700 kW. Thus, the numerical model is able to reproduce the designed heat recovery system operating parameters determined by theoretical correlations.

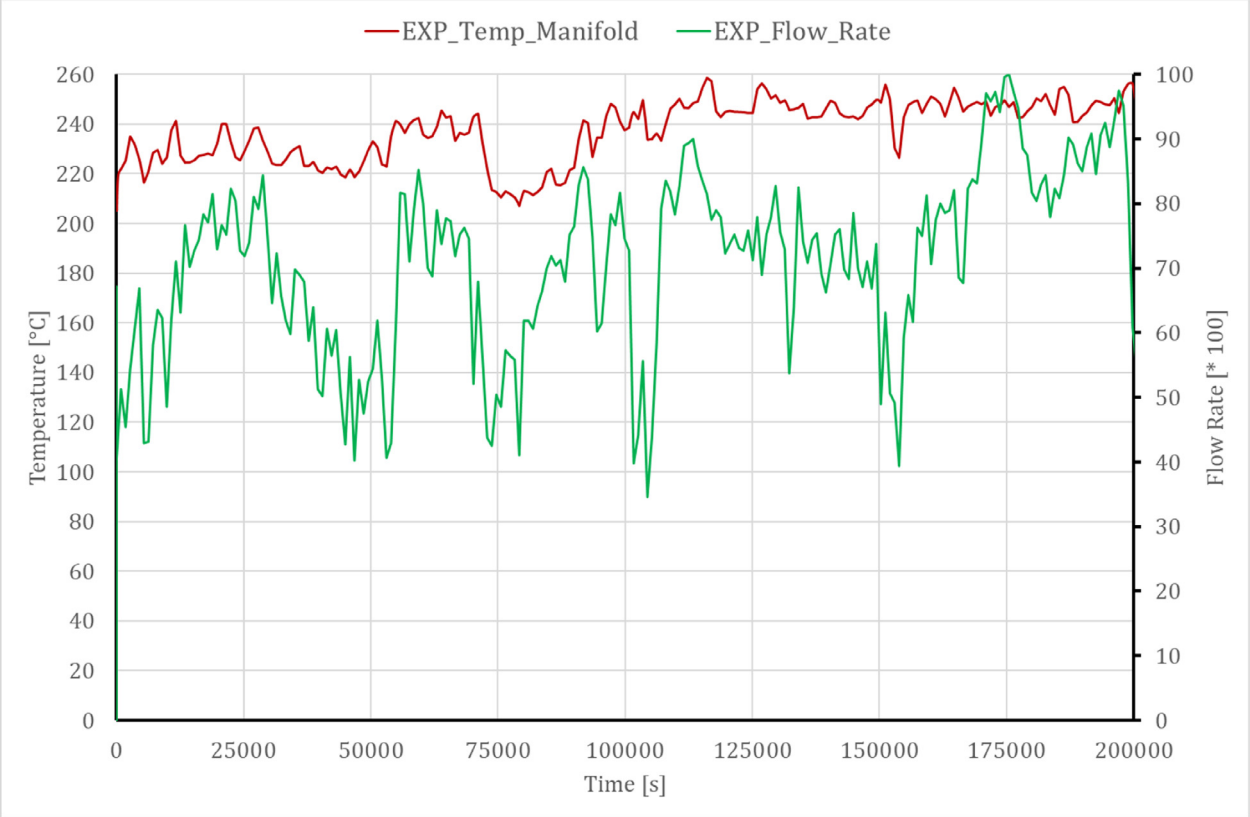

Fig. 11. Experimental temperature and flow rate of the exhaust at the manifold implemented in the numerical model as input data.

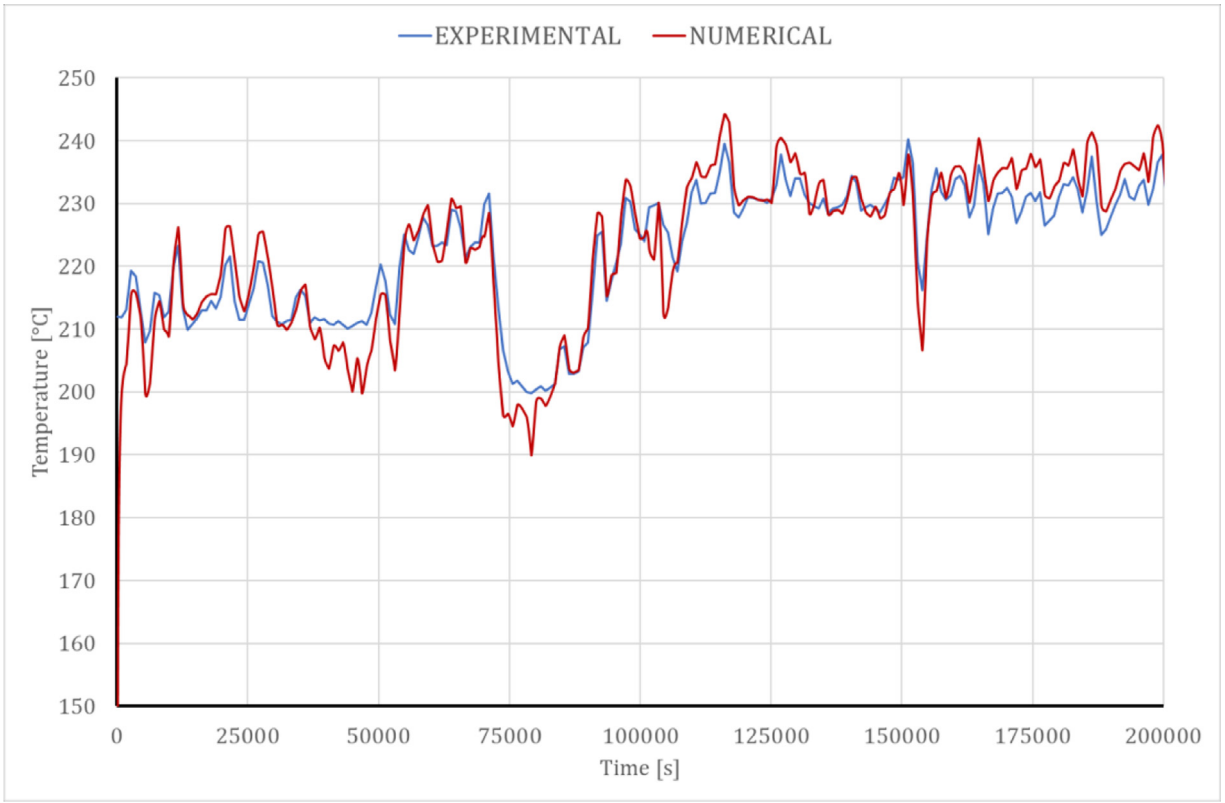

Fig. 12. Experimental and numerical temperature of the before the main stack.

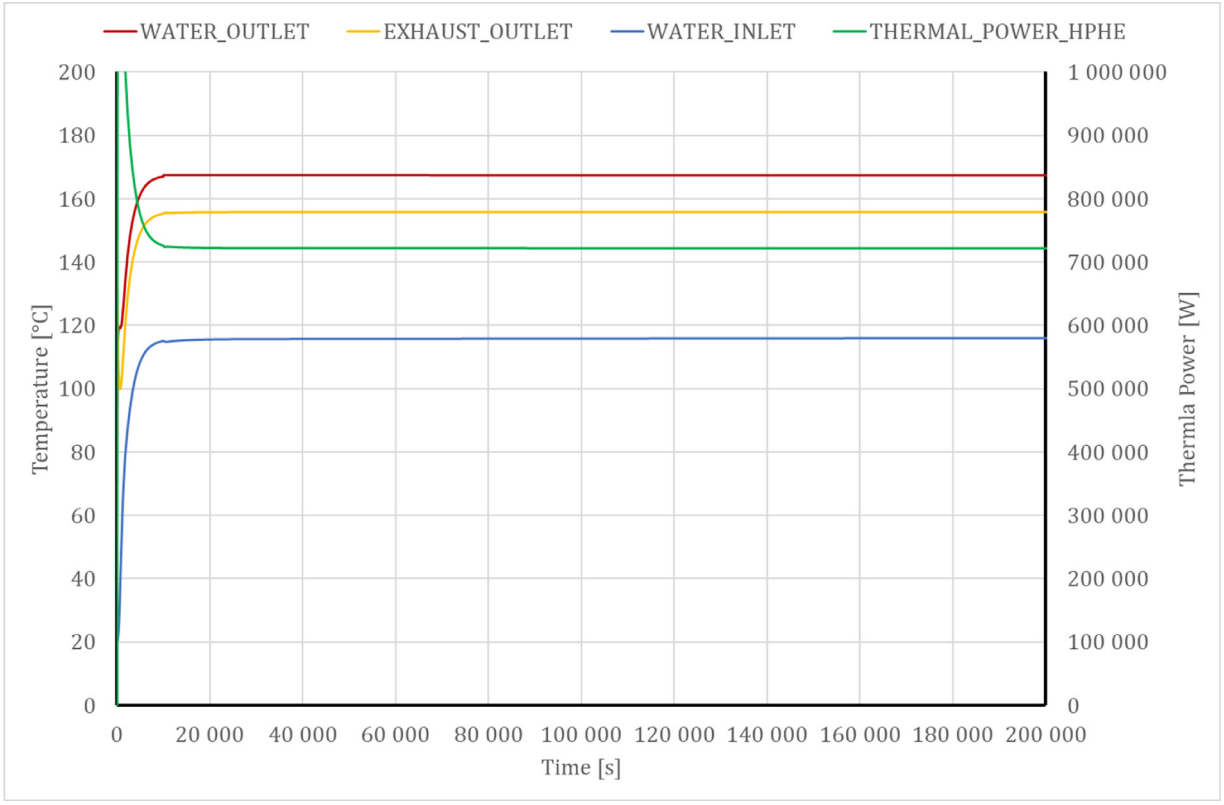

Fig. 13. Numerical temperature of the exhaust at the outlet of the HPHE (yellow line) and of the water at the inlet (blue line) and outlet (red line) of the HPHE. Thermal Power recovered by the HPHE (green line).

Control strategy sensitivity analysis

Once the numerical model has been validated against experimental data and theoretical correlations, the 0D/1D model has been used to simulate different working points of the heat recovery system under variable boundary conditions. Different simulations have been carried out to investigate the thermal performance of the system in situations that could occur during the real working conditions.

Case A-sensitivity analysis of spray dryer flow rate variation and bypass valve opening angle

In this scenario, the inputs of the exhaust gases have been kept equal to their designed value: 245°C and 100% (non-dimensional value for the flow rate). The pump rotational speed is maintained constant at the designed value of 2520 rpm.

The influence of two parameters have been analysed on the thermal behaviour of the system: the opening of the bypass of the evaporator section of the HPHE and a reduction of the flow rate of the spray dryer air (the secondary flows that recover the heat in the intermediate heat exchangers). In both the intermediate heat exchangers, a reduction in the air flow rate has been investigated: the air flow rate has been decreased from the nominal value of 100% (designed working condition) up to the 10% of the designed flow rates. In every simulation, the air flow rate in the intermediate heat exchangers has been reduced of a 10% with the respect to the nominal value (100%). Table 5 summarises the simulations carried out varying the air flow rate in the intermediate heat exchangers.

The influence of opening the bypass of the HPHE evaporator section has been investigated for every simulation reported in Table 5. In particular, different bypass angles have been considered starting from the bypass valve angle equal to 0 (completely closed) up to 90 (completely opened) varying the opening angle of 10 degrees every simulation. Thus, considering the simulation carried out varying the flow rate of the intermediate heat exchangers and the influence of the bypass opening valve, a matrix of 100 simulations is determined.

Fig. 14, Fig. 15 and Fig. 16 show the numerical results of the simulations' matrix carried out for this analysis, in particular, the temperature of the exhaust at the outlet of the HPHE and the temperature of the water stream at inlet and outlet of the condenser are presented. For each variable analysed, an operating 3D map and a table summarising the numerical results have been obtained to determine the working points of the heat recovery system considering the different openings of the bypass valve and the air flow rates in the intermediate heat exchangers simulated.

The predicted outlet temperature of the exhaust gases of the HPHE is shown in Fig. 14. It can be noticed, in the designed condition (100% flow rate to the spray dryer and bypass closed), the outlet

Table 5
Simulated scenarios varying the flow rate of the intermediate heat exchangers.

Simulation Number	Flow Rate of Intermediate HE#1 (% of designed flow rate)	Flow Rate of Intermediate HE#2 (% of designed flow rate)
1	100	100
2	90	90
3	80	80
4	70	70
5	60	60
6	50	50
7	40	40
8	30	30
9	20	20
10	10	10

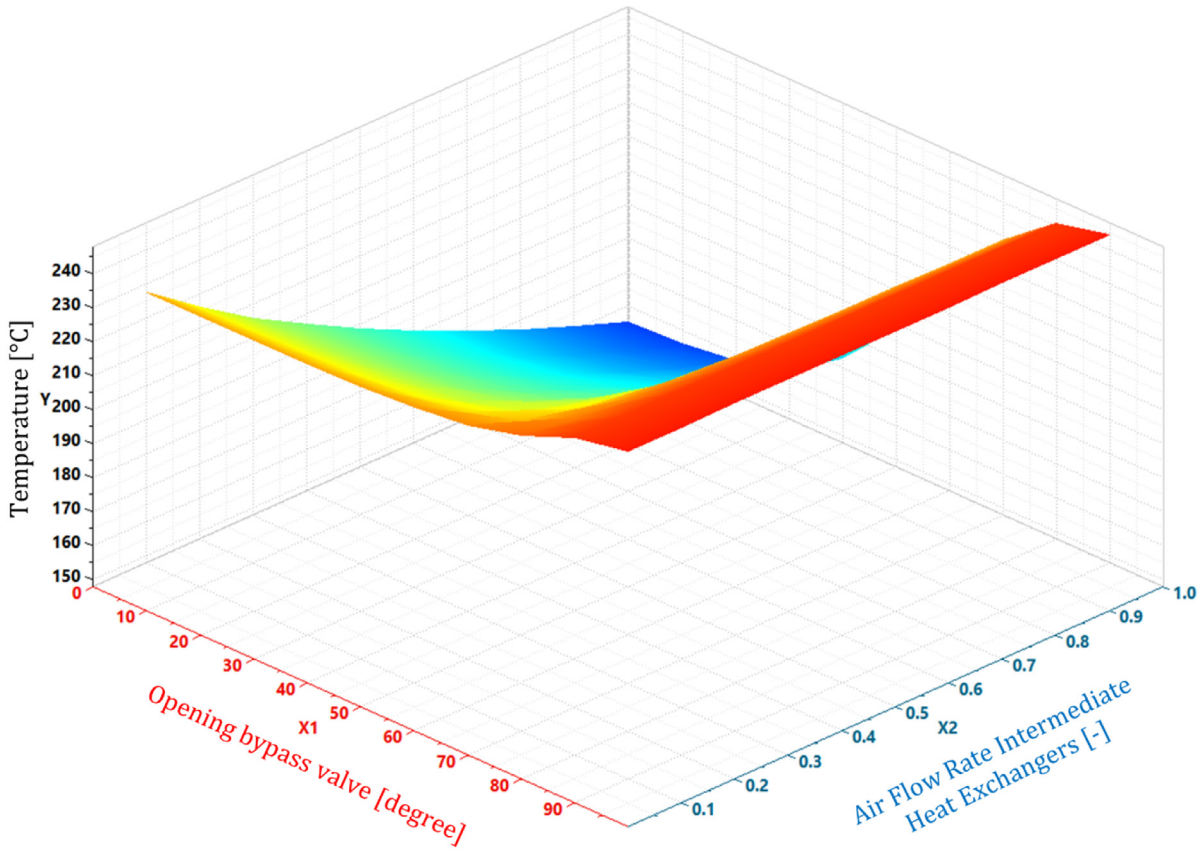

	Opening bypass valve angle [degree]									
Air Flow Rate Intermediate Heat Exchangers (%)	0	10	20	30	40	50	60	70	80	90
100%	155.6	156.1	158.4	163.5	173.1	188.8	209.4	228.9	241.2	244.8
90%	161.2	161.7	163.7	168.2	176.8	191.1	210.3	229.1	241.2	244.8
80%	167.3	167.7	169.5	173.4	180.9	193.6	211.3	229.3	241.2	244.8
70%	173.9	174.2	175.7	179.0	185.4	196.6	212.6	229.6	241.2	244.8
60%	181.0	181.3	182.5	185.2	190.5	200.0	214.2	229.9	241.2	244.8
50%	188.8	189.0	190.0	192.0	196.2	204.0	216.0	230.4	241.3	244.8
40%	197.3	197.5	198.0	199.5	202.7	209.5	218.4	231.0	241.4	244.8
30%	206.0	206.6	207.0	208.0	210.0	214.0	221.4	231.9	241.4	244.8
20%	216.5	216.7	217.0	217.4	218.6	221.0	225.3	233.0	241.4	244.8
10%	227.9	227.8	227.9	228.1	228.5	229.5	231.3	235.3	241.5	244.8

Fig. 14. Numerical temperature of the exhaust at the outlet of the HPHE varying the air flow rate in the intermediate heat exchangers (spray dryer) and the opening of the bypass valve in the exhaust flow.

temperature is 155°C. By increasing the opening of the bypass valve, a greater amount of the exhaust gases flows through the bypass and the heat recovery in the heat exchanger decreases. No heat recovery takes place when the bypass valve is completely opened, i.e. 90 degrees, because the exhaust completely bypasses the heat exchanger.

Furthermore, the increase in the exhaust gases temperature is determined also by the decrease in the air flow rate in the intermediate heat exchangers. A maximum temperature of 228°C can be reached when the air flow rate in the intermediate heat exchangers is at 10% of the designed value. A similar behaviour can be noticed for the water temperature at the inlet (Fig. 15) and at the outlet (Fig. 16) of the condenser section of the HPHE. Indeed, the temperature is approximately 115°C and 167°C at the inlet and outlet, respectively, in the designed working condition, i.e. 100% of the air flow rate in the intermediate heat exchanger and with the bypass completely closed. The temperature of the water (both at the inlet and outlet) decreases when opening the bypass valve. This leads to a lower amount of thermal energy recovered by the HPHE.

If the air flow rate in the intermediate heat exchangers decreases, the temperatures of the water increases. The opening of the bypass is necessary to keep the water temperatures in the desired range.

The temperature at the outlet of the HPHE is one of the main parameters that need to be monitored in order to avoid the acid content within the exhaust gases condensing. The opening of the exhaust bypass will be used to maintain the temperature in the desired range. The matrix of the simulations carried out has been used to determine the exhaust gases temperature increase per unit time (°C/s); this

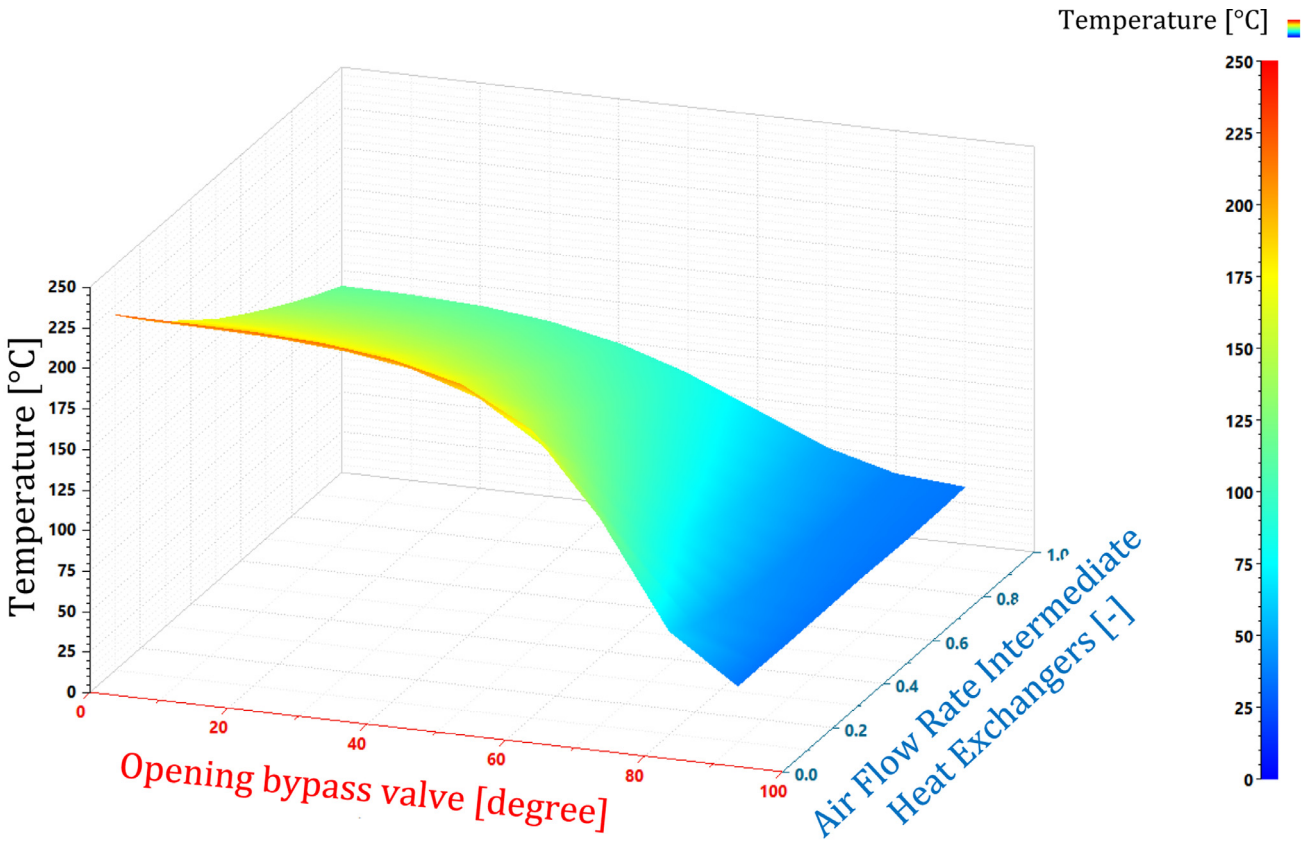

Air Flow Rate Intermediate Heat Exchangers (%)	Opening bypass valve angle [degree]									
	0	10	20	30	40	50	60	70	80	90
100%	114.7	114.2	112.2	107.8	99.5	85.8	67.5	49.8	38.4	35.08
90%	122.8	122.0	120.3	115.7	107.0	92.3	72.2	52.0	38.8	34.8
80%	131.6	131.0	129.0	124.3	115.2	99.6	77.7	54.9	39.5	34.8
70%	141.1	140.6	138.5	133.7	124.3	108.0	84.2	58.4	40.4	34.8
60%	151.4	150.9	148.8	144.0	134.6	117.7	92.0	62.7	41.6	34.8
50%	162.6	162.0	160.1	155.5	146.1	128.9	101.5	68.5	43.1	34.8
40%	174.9	174.4	172.2	168.2	159.2	142.1	113.4	76.1	45.3	34.8
30%	188.4	187.9	186.2	182.4	174.2	158.0	128.5	86.8	48.4	34.8
20%	203.0	202.8	201.5	198.3	191.5	177.2	149.0	102.9	53.7	34.8
10%	219.0	219.0	218.5	216.3	211.0	200.9	177.8	129.0	63.9	34.8

Fig. 15. Numerical temperature of the water at the inlet of the HPHE varying the air flow rate in the intermediate heat exchangers (spray dryer) and the opening of the bypass valve in the exhaust flow.

calculated value is fundamental for the tuning of the control strategy in order to open the bypass valve at the required angle when out of range parameters occur.

Fig. 17 shows the temperature gain in °C/s (y-axis) for the exhaust gases at the HPHE outlet per each spray drier mass flow rate and per each bypass valve opening angle simulated (x-axis). Analysing the curve at a random spray dryer flow rate, it is clearly visible that, as expected, the temperature gain increases with the increase of the bypass valve opening. For instance, with the 100% air flow rate curve, the temperature gain increases from 0.0003°C/s at 10 degrees bypass valve opening up to 0.23°C/s when the bypass is completely opened. For the same curve, when the bypass is opened at 20 degrees, the gain is 0.006°C/s which means approximately 3.6°C in ten minutes.

In addition to this, for a certain bypass valve opening, the temperature gain increases with the decrease of the air flow rate at the intermediate heat exchangers meaning less thermal energy is exploited when the air flow rate decreases. Thus, the water stream flows at the inlet of the condenser at a higher temperature, recovering less thermal energy in the HPHE condenser inlet and leading to an increase in the exhaust temperature at the outlet of the evaporator section.

Case B-sensitivity analysis of exhaust thermal power variation

The control strategy has been tested for two conditions that simulate different parameter fluctuations that could occur in the real system, namely an excess of or a decrease in thermal energy available in

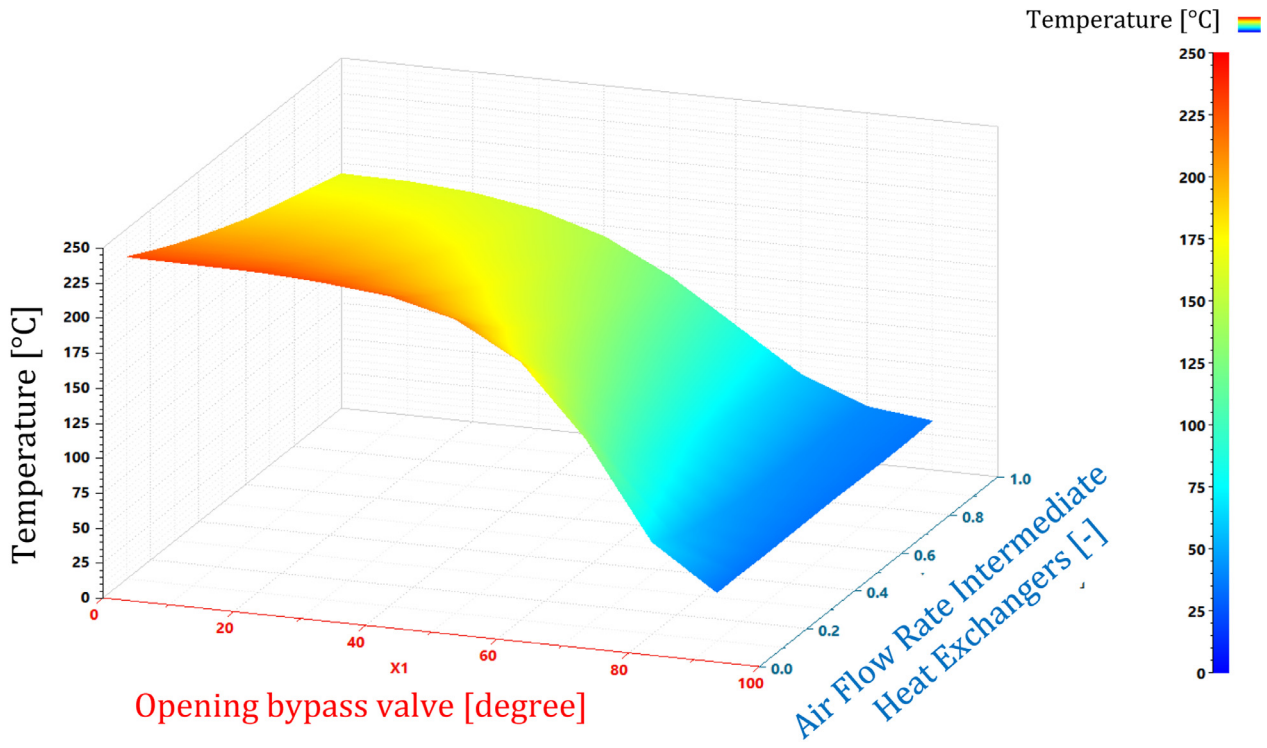

Air Flow Rate Intermediate Heat Exchangers (%)	Opening bypass valve angle [degree]									
	0	10	20	30	40	50	60	70	80	90
100%	167.6	166.8	163.5	156.0	142.0	119.0	88.5	59.0	40.8	35.1
90%	172.6	171.7	168.5	161.2	147.3	124.2	92.6	61.4	41.0	34.9
80%	177.9	177.0	174.0	166.9	153.2	130.0	97.5	64.0	41.7	34.8
70%	183.6	182.8	180.0	173.0	159.8	136.7	103.2	67.4	42.6	34.8
60%	189.8	189.0	186.2	179.8	167.1	144.4	110.2	71.6	43.8	34.8
50%	196.5	195.8	193.3	187.3	175.3	153.4	118.6	77.0	45.3	34.8
40%	203.8	203.2	201.0	195.6	184.7	163.9	129.2	84.3	47.3	34.8
30%	211.8	211.0	209.2	204.9	195.3	176.5	142.8	94.5	50.5	34.8
20%	220.6	220.0	218.7	215.2	207.5	191.8	160.5	109.2	55.8	34.8
10%	230.3	230.0	229.0	226.7	221.7	210.7	185.0	134.6	65.7	34.8

Fig. 16. Numerical temperature of the water at the outlet of the HPHE varying the air flow rate in the intermediate heat exchangers (spray dryer) and the opening of the bypass valve in the exhaust flow.

the exhaust gases. The first simulation is related to an excess of energy content in the exhaust. In particular, data characterised by a higher temperature and flow rate than the designed value are implemented as inputs to the numerical model. Finally, the second simulation concerns a temperature and a flow rate, and hence energy content, in the exhaust lower than within the designed values.

Fig. 18 shows the temperature and flow rate of the two out of range conditions simulated. The exhaust flow rate is normalized to the designed value in both cases. After a simulation time of 30,000 seconds where the input parameters are kept constant to the design values in both cases, the perturbations occur. In Fig. 18 (a) (simulation with higher energy content) the temperature and the flow rate of the exhaust reach 260°C and the 120%, respectively. In the simulation with the less energy content the temperature and flow rate decrease up to 210°C and 76%, see Fig. 18 (b). In these simulations the control strategy is activated; the speed of the pump is regulated to maintain the water temperature at the condenser outlet at 165°C.

If the variation of the water flow rate is not sufficient, a partial bypass of the evaporator will be operated in case of excess of thermal power in the exhaust while the bypass of one intermediate heat exchanger will be performed in the second simulation, i.e. decrease of thermal power in the exhaust gases.

In the following sections, the results of the two perturbations are reported.

Excess of thermal power in the exhaust gases

Fig. 19 shows the numerical results of the simulation for an excess of thermal power condition in the exhaust stream. The temperatures of two streams and the rotational speed of the pump are shown in Fig. 19 (a). When the source of the exhaust gases are in the designed condition (245°C and 100 % of the flow rate) the temperatures stabilise at the nominal conditions. Specifically, 155°C for the exhaust temperature at the outlet of the HPHE evaporator section, 115°C and

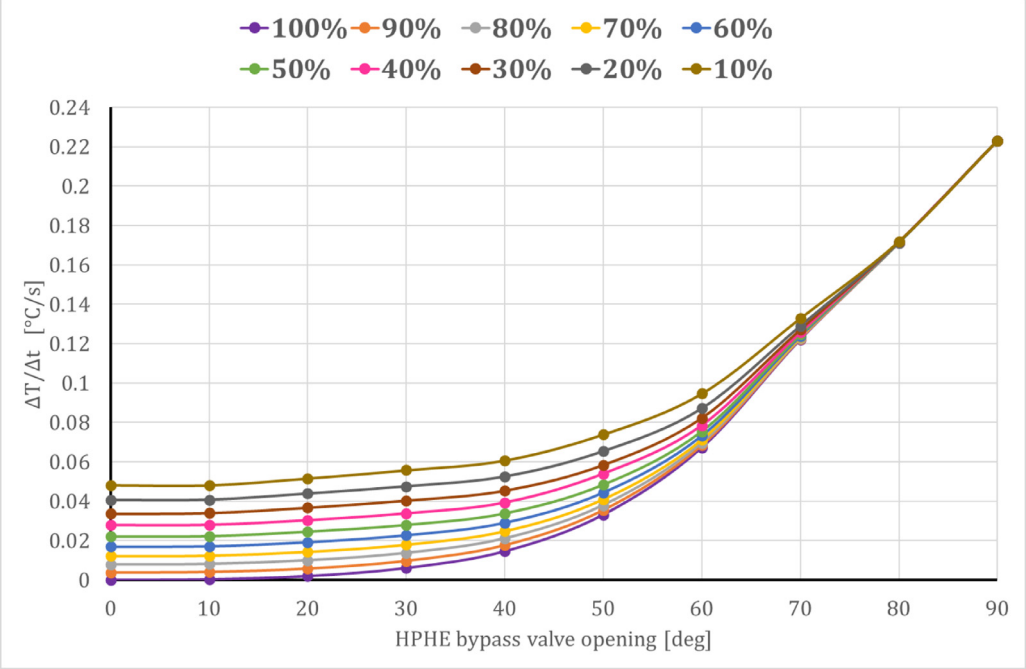

Fig. 17. Exhaust temperature gain per unit time [°C/s] under different bypass valve openings and spray dryer flow rates.

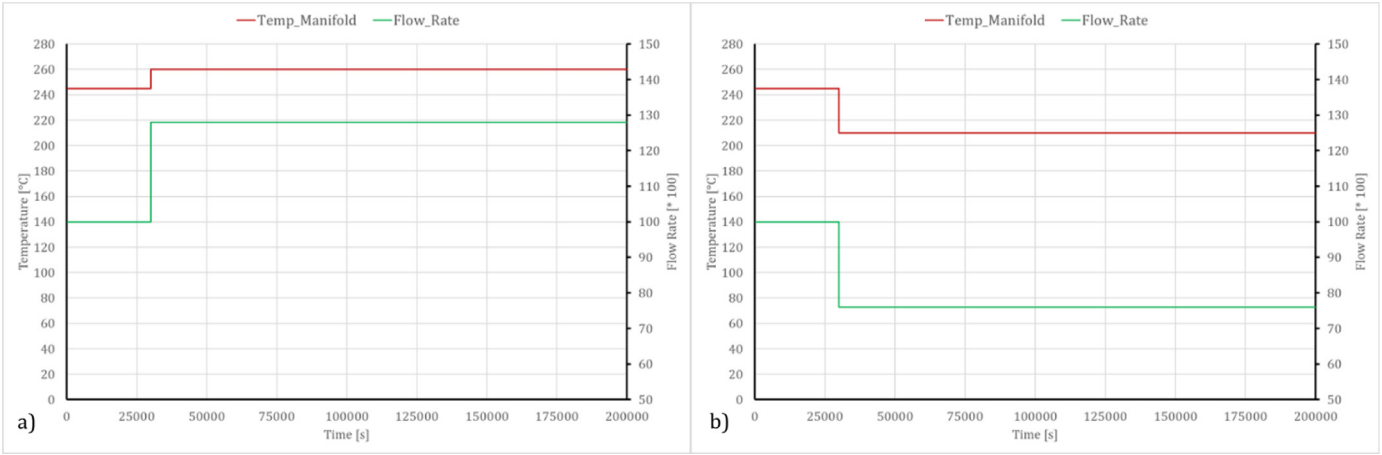

Fig. 18. (a) Experimental temperature and flow rate of the exhaust at the manifold implemented in the numerical model as input for the excess of thermal power. (b) The case for a decrease in available thermal power.

165°C for the water temperature at the inlet and outlet of the HPHE condenser section, respectively. The nominal conditions are reached also for the pump rotational speed, see Fig. 19 (a), and thermal power recovered, see Fig. 19 (b).

A major energy content increase in the exhaust (starting from 30,000 seconds) leads to an increase in thermal power recovered from the HPHE, that is approximately 14% more with respect to the thermal power recovered in the nominal conditions. Thus, an increase of the characteristic temperatures can be noticed; indeed, the exhaust gases temperature before exiting to the atmosphere is 181°C while the water stream temperatures registered are 135°C and 186°C at the inlet and outlet of the condenser respectively.

Fig. 19 (a) shows that the pump accelerates up to 3000 rpm when the perturbation occurs, but the increased water flow rate is not sufficient to maintain the temperature of the water at the desired temperature of 165°C. In response, the bypass valve operated at 50,000 seconds to reduce the energy content in the exhaust gases, opening to 40 degrees.

The thermal power recovered by the HPHE shown in Fig. 19 (b) decreases up to the nominal value, i.e. 700 kW and the water temperature at the outlet of the condenser stabilizes at 165°C. The opening of the bypass valve generates an increase of the exhaust temperature, i.e. 195°C; the increase in temperature of the exhaust is approximately 15°C in 20 minutes, which is very close to the rate shown in Fig. 17 for the same valve opening.

Decrease of thermal power in the exhaust gases

The results of the perturbation with the lower energy content in the exhaust with the respect to the nominal condition are shown in Fig. 20. The thermal behaviour of the system is the same as the one shown in the previous section when the designed conditions are simulated, up to 30,000 seconds. The decreased of the energy content in the exhaust, starting at 30,000 seconds, determines a lower thermal energy recovered by the HPHE: 550 kW with the respect to the 700 kW recovered in the nominal condition, see Fig. 20 (b). The control

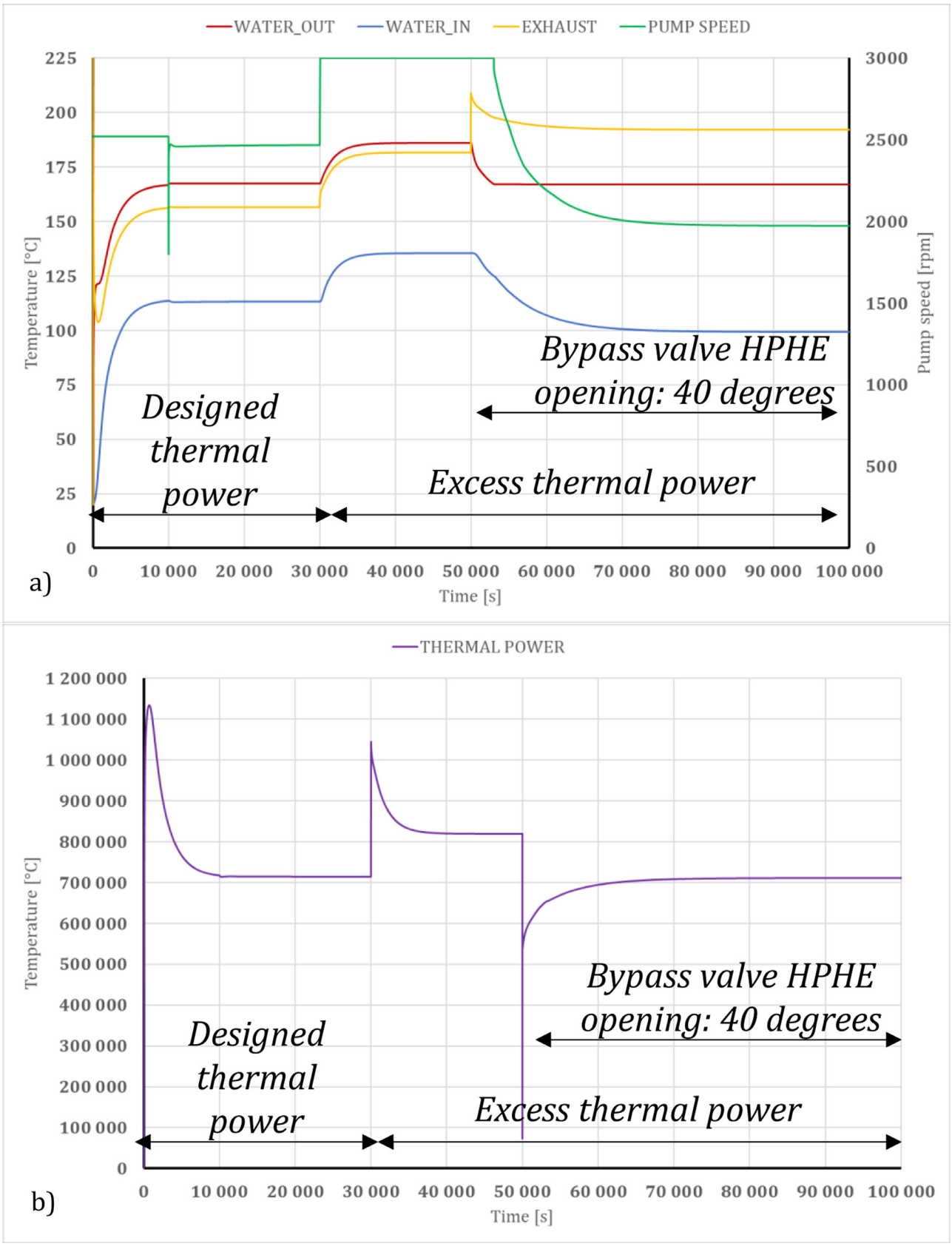

Fig. 19. (a) Numerical results for an excess thermal power condition. (b) Corresponding thermal power recovered by the HPHE.

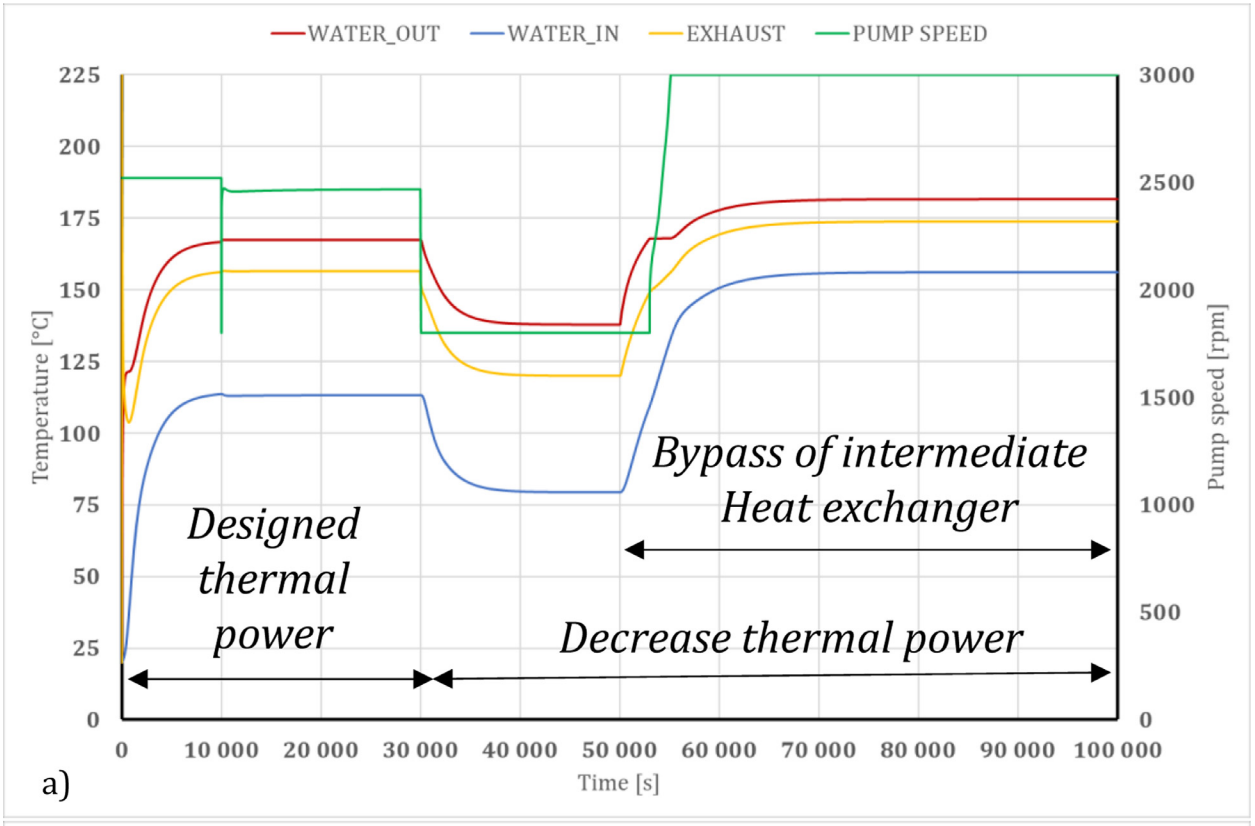

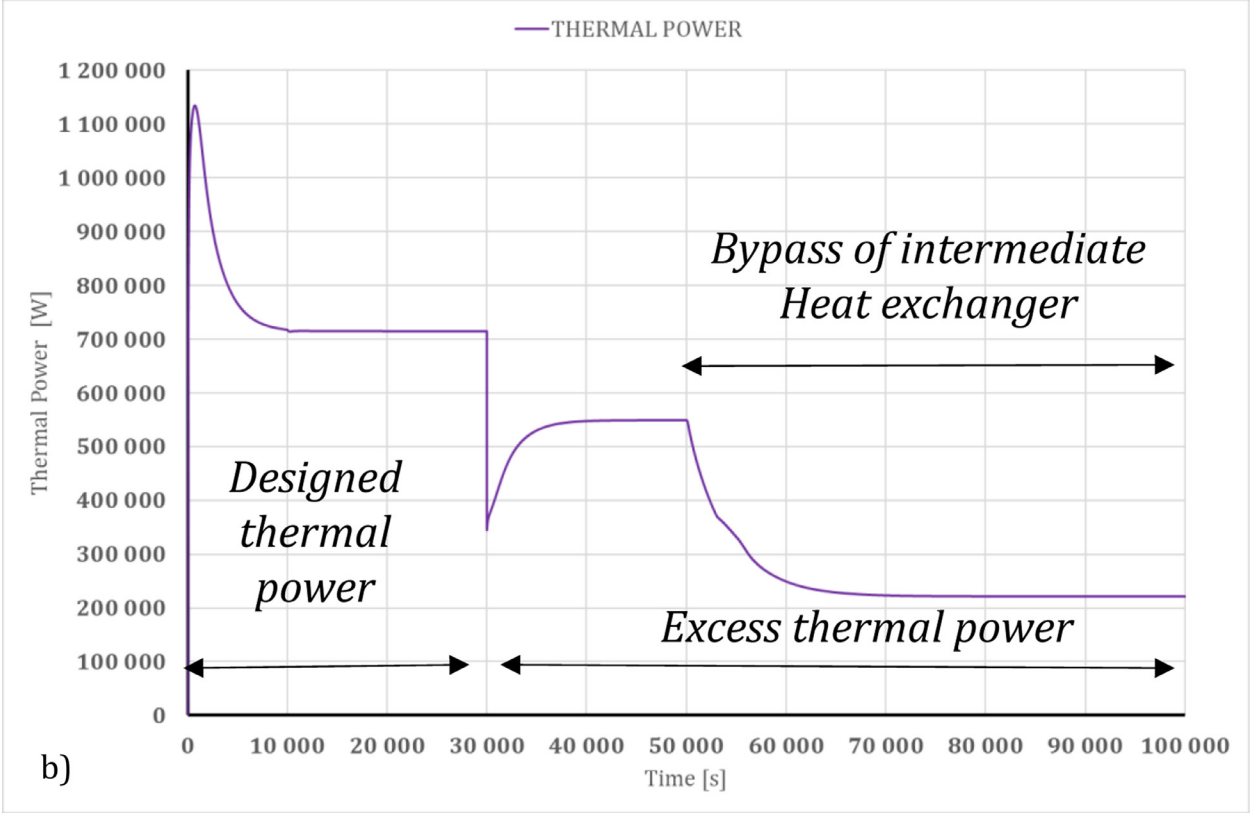

Fig. 20. (a) Numerical results for an insufficient thermal power condition. (b) Corresponding thermal power recovered by the HPHE.

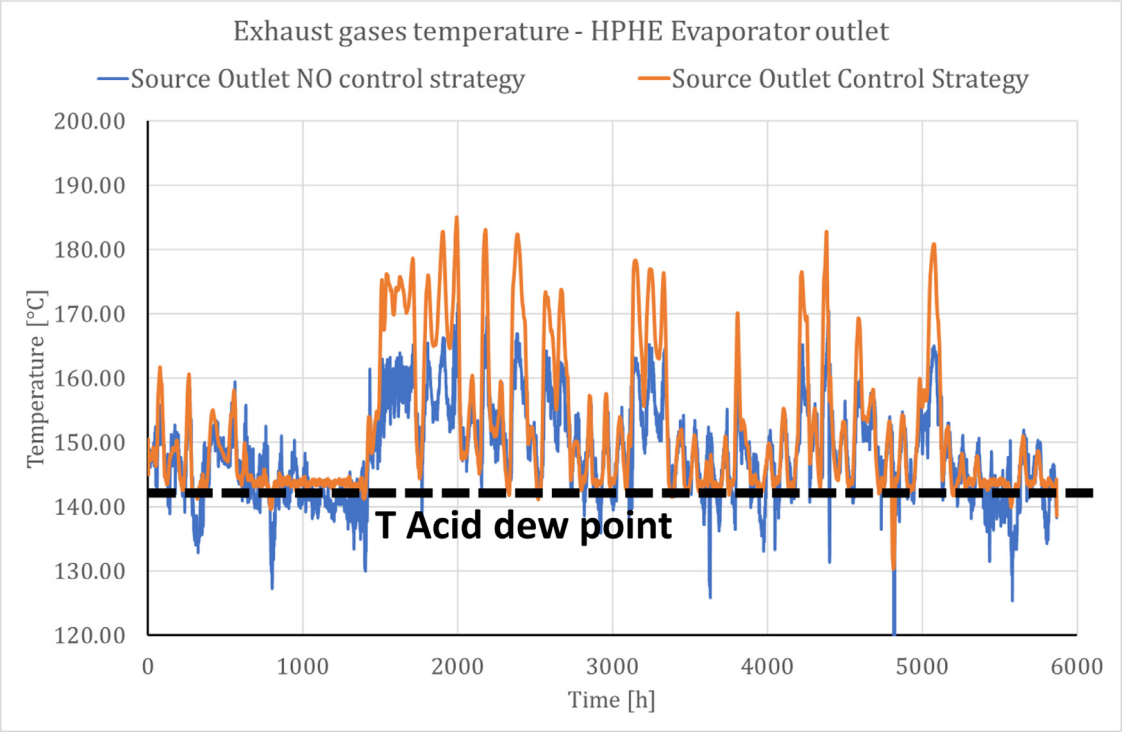

Fig. 21. Numerical results for a real test case. Temperature of the exhaust at the HPHE evaporator outlet when the control strategy is active and inactive.

strategy slows down the pump's speed when the perturbation is registered, i.e. 30,000 seconds, to decrease the water flow rate in the condenser but it is not sufficient to maintain the water temperature at 165°C. The water stabilizes at 137°C and 80°C at the inlet and outlet, respectively, while the exhaust gases temperature is 120°C, see Fig. 20 (a).

The solution to increase the characteristic temperature in the bypass of the intermediate heat exchanger is to exploit less thermal energy in the spray dryer. In response, at 50,000 seconds, the bypass of the main heat exchanger is performed. It can be seen from Fig. 20 (a) that the water and exhaust temperatures rise. The speed of the pump increases up to 3000 rpm to maintain the water outlet at 165° C.

Application of the control strategy to a real test case

In this paragraph, the performance of the control strategy presented in Paragraph 3.3 has been tested with fluctuating experimental data, i.e. the same input values used to run the numerical simulation in Paragraph 3.1.2. The results of the control strategy sensibility analysis reported above highlights the requirement of an additional component in the control loop: a Proportional-Integral-Derivative controller (PID) that aims at minimizing the error between the calculated temperature at the evaporator outlet and the setpoint temperature, i.e. 155°C. When the exhaust thermal energy in the exhaust is larger than the designed value (larger flowrate or temperature in the exhaust), the PID controller opens the exhaust bypass valve decreasing the exhaust flowrate that flow through the HPHE unit. The following figures compare the outlet temperatures (both at the evaporator and the condenser sections) when the control strategy is active and when it is not, i.e. results of the simulation shown in Paragraph 3.1.2.

In Fig. 21, it is shown that the exhaust temperature at the HPHE outlet when the control strategy is active fluctuated between 140 and 180°C. Thus, the temperature of the exhaust is maintained above the acid dew point temperature. When the control strategy is inactive, the temperature of the exhaust reached 125°C that leads to acid condensation, please refer to Paragraph 3.1.2. Similarly, the water temperature seen at the outlet of the condenser benefits from the implementation of the control strategy; indeed, the water temperature reaches a maximum of 180°C preventing any vapourisation of the water stream, see Fig. 22. The control strategy is able to reduce the water temperature of 15-20°C with the respect to the results of the simulation without the control strategy.

Conclusion

In this paper, the energy efficiency enhancement due to the heat recovery from the exhaust gases of ceramic furnaces has been evaluated. The application of a HPHE to improve the energy efficiency and to reduce the environmental impact of a ceramic process is investigated. In the study, a lumped and distributed numerical model of the exhaust piping from the outlet of the furnaces to the main stack has been constructed and validated against experimental data. The agreement between the calculations and the measurements showed good agreement when investigating the thermal losses along the exhaust gases piping.

A TRNSYS analysis of the proposed HPHE installation without a control strategy showed the necessity to introduce one, due to the high fluctuations in the exhaust temperature and mass flow rate, in order to a steadier state required to maintain the quality of the product through the spray drying process. Furthermore, there were times when the temperature of the exhaust dropped below the due point of some aggressive condensable gases. This could not occur in the real scenario to prevent fouling and corrosion issues, and to ensure the equipment introduced has longevity of life.

Afterward, a numerical model of the entire heat recovery system has been developed to investigate the thermal performance of the system and to tune the control strategy of the heat recovery circuit. The 0D/1D model accounts for the main components of the circuit: the HPHE and the heat transfer fluid closed loop circuit with specific models for the pump and the heat exchangers that exploit the energy

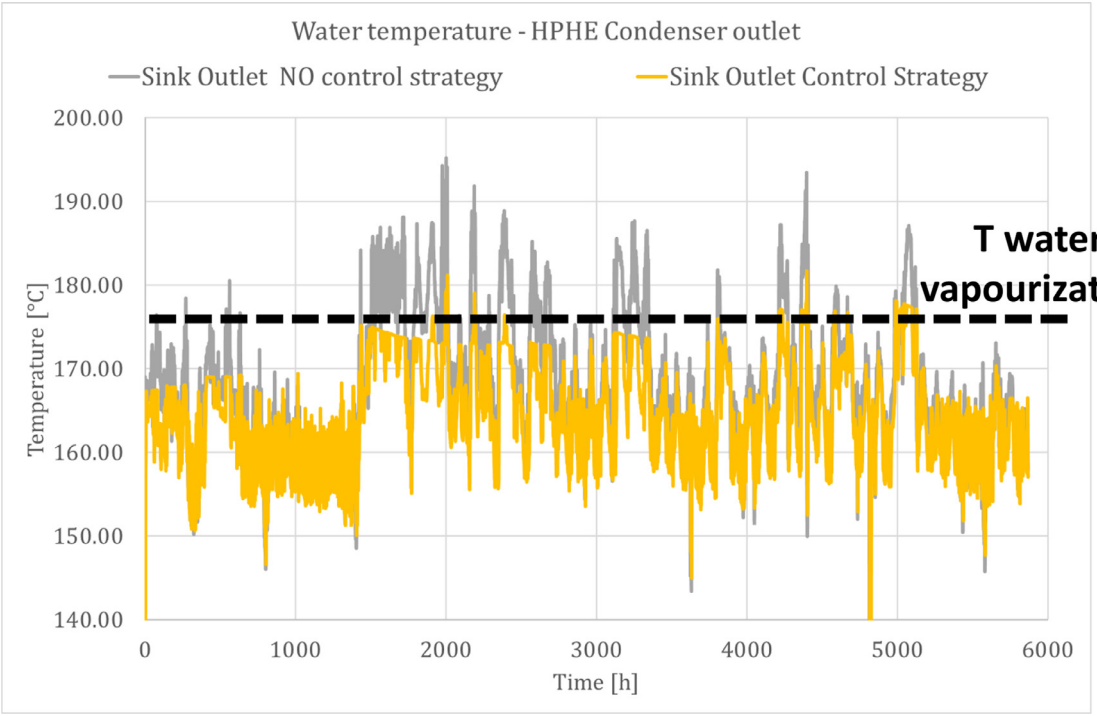

Fig. 22. Numerical results for a real test case. Temperature of the water at the HPHE condenser outlet when the control strategy is active and inactive.

recovered in the heat sink. The results of the proposed numerical model are validated against theoretical correlations under the nominal working condition designed for the system.

3D operating maps are determined to investigate the influence of the variation of the spray-dryer flow rate and of the opening of the bypass valve on the thermal performance of the heat recovery system under the nominal working conditions, i.e. designed exhaust temperature and flowrate.

Furthermore, the control strategy behaviour is investigated under two different perturbations: excess and decrease of thermal energy content in the exhaust. The numerical analysis demonstrated that it is necessary to open the bypass valve to 40 degrees when the maximum spike in the exhaust flow rate and temperature is registered, while a bypass of the main heat exchanger is necessary when the energy content of the exhaust is at a minimum.

Finally, the control strategy is tested with real fluctuating conditions. The numerical investigation showed that acid condensation in the primary stream is prevented since the temperature of the exhaust is maintained above 140°C, i.e. acid dewpoint temperature. Similarly, the water temperature registered at the condenser outlet is lower than 180°C: the secondary stream vapourisation is avoided even under an excess of thermal energy in the exhaust.

Declaration of Competing Interest

The authors declare that they have no known competing financial interests or personal relationships that could have appeared to influence the work reported in this paper.

Acknowledgements

The presented work is part of HEAT PIPE TECHNOLOGY FOR THERMAL ENERGY RECOVERY IN INDUSTRIAL APPLICATIONS — ETEKINA project. The project has received funding from the European Union's Horizon 2020 research and innovation programme under grant agreement N° 768772.

References

[1] B. Egilegor, H. Jouhara, J. Zuazua, F. Al-Mansour, K. Plesnik, L. Montorsi, L. Manzini, ETEKINA: analysis of the potential for waste heat recovery in three sectors: aluminium low pressure die casting, steel sector and ceramic tiles manufacturing sector, Int. J. Thermofluids 1 (2020) 100002 2020, doi: 10.1016/j.ijft.2019.100002.
[2] J. Malinauskaite, H. Jouhara, B. Egilegor, F. Al-Mansour, L. Ahmad, M. Pusnik, Energy efficiency in the industrial sector in the EU, Slovenia, and Spain, Energy 208 (2020) 118398, doi: 10.1016/j.energy.2020.118398.
[3] J. Malinauskaite, H. Jouhara, L. Ahmad, M. Milani, L. Montorsi, M. Venturelli, Energy efficiency in industry: EU and national policies in Italy and the UK., Energy 172 (2019) 255–269, doi: 10.1016/j.energy.2019.01.130.
[4] Confindustria Ceramica Report (2016).
[5] H. Jouhara, N. Khordehgah, S. Almahmoud, B. Delpech, A. Chauhan, S.A. Tassou, Waste heat recovery technologies and applications, Thermal Sci. Eng. Progr. 6 (2018) 268–289, doi: 10.1016/j.tsep.2018.04.017.
[6] Daniel Brough, Hussam Jouhara, The aluminium industry: a review on state-of-the-art technologies, environmental impacts and possibilities for waste heat recovery, Int. J. Thermofluids (2020), doi: 10.1016/j.ijft.2019.100007.
[7] European Commission, Reference Document in the Ceramic Manufacturing Industry, 2007.
[8] A. Mezquita, J. Boix, E. Monfort, G. Mallol, 1 Appl. Thermal Eng. 65 (1-2) (2014) 102–110, doi: 10.1016/j.applthermaleng.2014.01.002.
[9] C. Agrafiotis, T. Tsoutsos, Energy saving technologies in the European ceramic sector: a systematic review, Appl. Thermal Eng. 21 (12) (2001) 1231–1249, doi: 10.1016/S1359-4311(01)00006-0.
[10] B. Peris, J. Navarro-Esbrí, F. Molés, A. Mota-Babiloni, Experimental study of an ORC (organic Rankine cycle) for low grade waste heat recovery in a ceramic industry, Energy 85 (2015) 534–542, doi: 10.1016/j.energy.2015.03.065.
[11] M. Milani, L. Montorsi, M. Stefani, R. Saponelli, M. Lizzano, Numerical analysis of an entire ceramic kiln under actual operating conditions for the energy efficiency improvement, J. Environ. Manag. 203 (2017) 1026–1037, doi: 10.1016/j.jenvman.2017.03.076.
[12] M. Milani, L. Montorsi, G. Storchi, M. Venturelli, D. Angeli, A. Leonforte, D. Castagnetti, A. Sorrentino, Experimental and numerical analysis of a liquid aluminium Injector for an Al-H2O based hydrogen production system, Int. J. Thermofluids (2020) 100018, doi: 10.1016/j.ijft.2020.100018.
[13] A-M.Nuñez Vega, B. Sturm, W. Hofacker, Simulation of the convective drying process with automatic control of surface temperature, J. Food Eng. 170 (2016) 16–23, doi: 10.1016/j.jfoodeng.2015.08.033.
[14] P. Bunyawanichakul, G.J. Walker, J.E. Sargison, P.E. Doe, Modelling and simulation of paddy grain (rice) drying in a simple pneumatic dryer, Biosyst. Eng. 96 (3) (2007) 335–344, doi: 10.1016/j.biosystemseng.2006.11.004.
[15] M. Ramadan, S. Ali, H. Bazzi, M. Khaled, New hybrid system combining TEG, condenser hot air and exhaust airflow of all-air HVAC systems, Case Stud. Thermal Eng. 10 (2017) 154–160, doi: 10.1016/j.csite.2017.05.007.

[16] Y. Luo, L. Zhang, Z. Liu, J. Wu, Y. Zhang, Z. Wu, Numerical evaluation on energy saving potential of a solar photovoltaic thermoelectric radiant wall system in cooling dominant climates, Energy 142 (2018) 384–399, doi: 10.1016/j.energy.2017.10.050.
[17] D. Brough, A. Mezquita, S. Ferrer, C. Segarra, A. Chauhan, S. Almahmoud, N. Khordehgah, L. Ahmad, D. Middleton, H.I. Sewell, H. Jouhara, An experimental study and computational validation of waste heat recovery from a lab scale ceramic kiln using a vertical multi-pass heat pipe heat exchanger, Energy 208 (2020) 118325, doi: 10.1016/j.energy.2020.118325.
[18] H. Mroue, J.B. Ramos, L.C. Wrobel, H. Jouhara, Experimental and numerical investigation of an air-to-water heat pipe-based heat exchanger, Appl. Thermal Eng. 78 (2015) 339–350, doi: 10.1016/j.applthermaleng.2015.01.005.
[19] J. Ramos, A. Chong, H. Jouhara, Experimental and numerical investigation of a cross flow air-to-water heat pipe-based heat exchanger used in waste heat recovery, Int. J. Heat Mass Transf. 102 (2016) 1267–1281, doi: 10.1016/j.ijheatmasstransfer.2016.06.100.
[20] M. Milani, L. Montorsi, S. Terzi, Numerical analysis of the heat recovery efficiency for the post-combustion flue gas treatment in a coffee roaster plant., Energy 141 (2017) 729–743, doi: 10.1016/j.energy.2017.09.098.
[21] B. Delpech, M. Milani, L. Montorsi, D. Boscardin, A. Chauhan, S. Almahmoud, B. Axcell, H. Jouhara, Energy efficiency enhancement and waste heat recovery in industrial processes by means of the heat pipe technology: Case of the ceramic industry, Energy 158 (2018) 656–665, doi: 10.1016/j.energy.2018.06.041.
[22] H.O. Gómez, M.C. Calleja, L.A. Fernández, A. Kiedrzyńska, R. Lewtak, Application of the CFD simulation to the evaluation of natural gas replacement by syngas in burners of the ceramic sector, Energy 185 (2019) 15–27, doi: 10.1016/j.energy.2019.06.064.
[23] H. Ershadi, A. Karimipour, Present a multi-criteria modeling and optimization (energy, economic and environmental) approach of industrial combined cooling heating and power (CCHP) generation systems using the genetic algorithm, case study: a tile factory, Energy 149 (2018) 286–295, doi: 10.1016/j.energy.2018.02.034.
[24] M. Milani, L. Montorsi, M. Venturelli, J.M. Tiscar, J. García-Ten, A numerical approach for the combined analysis of the dynamic thermal behaviour of an entire ceramic roller kiln and the stress formation in the tiles, Energy 177 (2019) 543–553, doi: 10.1016/j.energy.2019.04.037.
[25] Heat pipe technology for thermal energy recovery in industrial applications (ETEKINA), Research and Innovation Action, European Union. Grant agreement N° 768772.
[26] D. Brough, J. Ramos, B. Delpech, et al., Development and validation of a TRNSYS type to simulate heat pipe heat exchangers in transient applications of waste heat recovery, Int. J. Thermofluids (2020) in press.
[27] Simcenter AMESim 2019 User Guide.